Electronic Supplementary Material (ESI) for ChemComm.

Supporting Information

Ligand Architecture for Triangular Metal Complexes: A High Oxidation State Ni_3 Cluster with Proximal Metal Arrangement

Manar M. Shoshani and Theodor Agapie

Department of Chemistry and Chemical Engineering, California Institute of Technology, 1200 E. California Blvd. MC 127-72, Pasadena, CA 91125, USA

*E-mail: agapie@caltech.edu

Experimental

General Considerations

All synthetic procedures were performed under a nitrogen-atmosphere M. Braun glove box or using Schlenk line techniques with nitrogen gas. All glassware was oven-dried and kept under active vacuum prior to use. Diethyl ether, tetrahydrofuran (THF), toluene, hexanes, and pentane solvents were purified by sparging with nitrogen and then passing through a column of activated A2 alumina into sealed containers, degassed under active vacuum and stored over activated molecular sieves prior to use. C_6D_6(Cambridge Isotope Laboratories) was distilled from a Na/Benzophenone pot and kept over molecular sieves prior to use. CD_3CN (Cambridge Isotope Laboratories) was distilled from CaH_2 and kept over activated molecular sieves prior to use. The syntheses of tris-3,5-di-tert-butylphenol phosphine[1], 2-bromo-4,6-di-tert-butylphenol[2] and decamethyl ferrocenium triflate[3] were previously reported. *o*-hydroxylamine-sulfonic acid, and 2-4-di-tert-butylphenol, decamethylferrocene, and Cp^*_2FeOTf were purchased from Sigma-Aldrich and used as received. $NiBr_2$.DME was purchased from Alfa Aesar and dried by warming to 70 °C under vacuum. PCl_3 was purchased from Sigma Aldrich and distilled prior to use. NMR spectra were recorded on a Varian 400 MHz Spectrometer. EPR spectra were obtained by freezing 2-MeTHF solutions of [**4**] = 2mM, using a Bruker EMX spectrometer. Elemental analysis was performed using a PerkinElmer 2400 Series II CHN Elemental Analyzer. Cyclic voltammograms were recorded with a Pine Instrument Company AFCBP1 bipotentiostat using the AfterMath software package. All measurements were performed in a three electrode cell, which consisted of (1) a glassy carbon working electrode, (2) a Pt wire counter electrode, and (3) a Ag wire reference electrode. Dry solvent that contained 0.1 M ^{n}Bu4NPF6 was employed as the electrolyte solution for all electrochemical measurements. All electrochemical measurements were performed at room temperature in an M. Braun nitrogen filled glovebox. The ferrocene/ferrocenium (Fc/Fc+) redox couple was used as an internal standard for all

measurements. X-ray diffraction data was collected at 100 K on a Bruker PHOTON100 CMOS based diffractometer (microfocus sealed X-ray tube, Mo Kα (λ) = 0.71073 Å or Cu Kα (λ) = 1.54178 Å). All manipulations, including data collection, integration, and scaling, were carried out using the Bruker APEXII software. Absorption corrections were applied using SADABS. Structures were solved by direct methods using XS (incorporated into SHELXTL) and refined by using ShelXL least squares on Olex2-1.2.7 to convergence. All non-hydrogen atoms were refined using anisotropic displacement parameters. Hydrogen atoms were placed in idealized positions and were refined using a riding model. Most crystals included solvent-accessible voids that contained disordered solvent. Additional two-site disorder was observed on the tert-butyl groups of compounds **3** and **4**. For both the solvent and the tert-butyl groups, disorder was modelled successfully.

Synthesis of Tris(3,5-di-tert-butyl-2-phenol)-iminophosphorane hydrosulfate (2): To a solution of the tris(3,5-di-tert-butyl-2-phenol)-phosphine (9.06 g, 14 mmol) in toluene (150mL) was added a degassed solution of *o*-hydroxyl amine sulfonic acid (1.58 g, 14 mmol, 1 equiv.) in methanol (50 mL), via cannula transfer. After stirring at room temperature for 15 minutes, all volatiles were removed in *vacuo*. The resulting mixture was then extracted in toluene (100 mL) and filtered through a pad of Celite. The solution was evaporated to afford the desired product (9.15 g, 86%). ^{1}H NMR (400 MHz, C_6D_6): δ 9.65 (broad s, 3H, OH), 7.67 (d, $^{4}J_{HH}$ = 2.2 Hz, 3H, Ph*H*), 6.81 (dd, $^{3}J_{HP}$ = 17.2 Hz, $^{4}J_{HH}$ = 2.2 Hz, 3H, Ph*H*), 6.01 (broad s, 2H, NH_2), 1.47 (s, 27H, ^{t}Bu), 1.01 (s, 27H, ^{t}Bu). ^{31}P{^{1}H} NMR (121 MHz, C_6D_6): δ 45.0 (s, 1P). ^{13}C{^{1}H} NMR (101 MHz, C_6D_6): δ 30.27 (s, 3C, CH(CH$_3$)$_3$), 31.17 (s, 3C, CH(CH$_3$)$_3$), 34.39 (s, 1C, CH(CH$_3$)$_3$), 35.51 (d, $^{4}J_{CP}$ = 1.7 Hz), 110.59 (s, 1C, Aryl-C), 111.65 (s, 1C, Aryl-C), 131.45 (s, 1C, Aryl-C), 141.19 (d, $^{2}J_{CP}$ = 7.0 Hz, 1C, Aryl-C), 144.38 (d, $^{1}J_{CP}$ = 14.1 Hz, 1C, Aryl-C), 157.98 (d, $^{2}J_{CP}$ = 2.2 Hz, 1C, Aryl-C). Anal. Calcd. (%) for $C_{42}H_{66}NO_7PS$: C, 66.37; H, 8.75; N, 1.84. Experimental: C, 66.11; H, 8.10; N, 1.59.

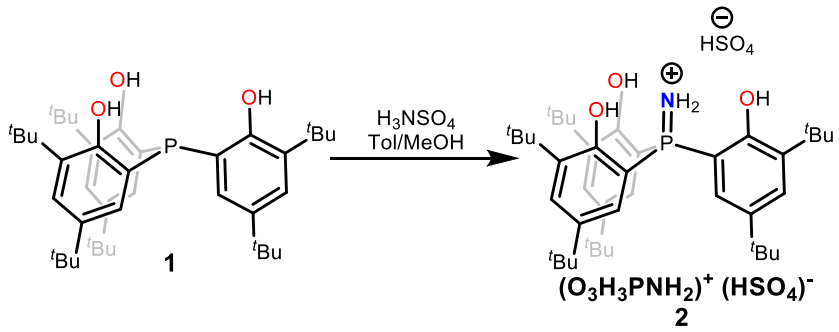

Synthesis of 3-DME: To a solution of **2** (300 mg, 0.395 mmol) in THF (10 mL) was added a solution of potassium tert-butoxide (292 mg, 2.607 mmol, 6.6 equiv.) in THF (5 mL) and was stirred at room temperature for 2 h. The solution was then frozen and subsequently added to a thawing stirring solution of $NiBr_2DME$ (177 mg, 0.593 mmol, 1.5 equiv.) in THF (20 mL). The dark yellow suspension was warmed to room temperature and stirred for 2.5 h at which point all volatiles were removed in vacuo. The residue was triturated with n-hexanes (3 x 10mL) and then extracted with toluene (20 mL) and filtered through a plug of Celite. The solution was then concentrated and was left at -40 °C for 24 h to afford dark yellow block crystals. To obtain single-crystals suitable for X-Ray diffraction, complex **3-DME** was dissolved in 1 mL of benzene and transferred a 4 mL vial. This vial was then inserted into a 20 mL vial with 4 mL of hexamethyldisiloxane. Single crystals of **3-HMDSO** suitable for X-Ray diffraction were grown over the course of 48 hours. (140 mg, 42% yield). ^{1}H NMR (400 MHz, C_6D_6): δ 7.47 (s, 4H, Ph*H*), 7.40 (s, 2H, Ph-H), 6.56 (d, $^3J_{HP}$ = 16.2 Hz, 4H, Ph*H*), 6.48 (d, $^3J_{HP}$ = 16.0 Hz, 2H, Ph*H*), 3.01 (s, 6H, OCH_3), 3.00 (s, 4H, OCH_2), 1.82 (s, 18H, ^{t}Bu), 1.60 (s, 18H, ^{t}Bu), 1.49 (s, 18H, ^{t}Bu), 1.16 (s, 36H, ^{t}Bu), 1.12 (s, 18H, ^{t}Bu). ^{31}P{^{1}H} NMR (121 MHz, C_6D_6): δ 27.9 (s, 2P). ^{13}C{^{1}H} NMR (100.8 MHz, C_6D_6): δ 30.60 (s, 6C, $CH(CH_3)_3$), 30.78 (s, 6C, $CH(CH_3)_3$), 31.66 (s, 6C, $CH(CH_3)_3$), 31.72 (s, 6C, $CH(CH_3)_3$), 31.75 (s, 6C, $CH(CH_3)_3$), 34.02 (s, 4C, $CH(CH_3)_3$), 34.10 (s, 2C, $CH(CH_3)_3$), 36.35 (s, 2C, $CH(CH_3)_3$), 36.71 (s, 2C, $CH(CH_3)_3$), 36.73 (s, 2C, $CH(CH_3)_3$), 58.81 (s, 2C, OCH_3) 71.46 (s, 2C, OCH_2CH_2O), 105.11 (s, 2C, Aryl-C), 106.10 (s, 2C, Aryl-C), 109.67 (s, 2C, Aryl-C), 110.64 (s, 2C, Aryl-C), 112.70 (s, 2C, Aryl-C), 113.71 (s, 2C, Aryl-C), 111.65 (s, 1C, Aryl-C), 127.25 (s, 2C, Aryl-C), 127.29 (s, 2C, Aryl-C), 127.55 (s,

2C, Aryl-C), 133.53 (m, 2C, Aryl-C), 134.29 (m, 2C, Aryl-C), 135.60 (m, 2C, Aryl-C), 141.47 (m, 2C, Aryl-C), 141.88 (m, 4C, Aryl-C), 168.34 (s, 2C, Aryl-C), 168.98 (s, 2C, Aryl-C), 169.25 (s, 2C, Aryl-C). Anal. Calcd. (%) for $C_{88}H_{130}N_2O_8P_2Ni_3K_2$: C, 63.66; H, 7.89; N, 1.69. Experimental: C, 63.07; H, 7.94; N, 1.66.

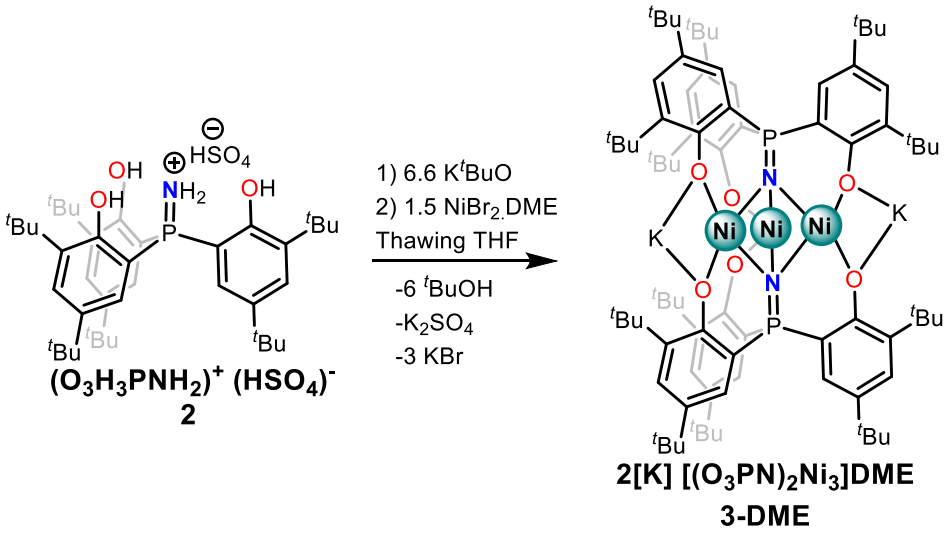

Synthesis of 4: To a solution of **3-DME** at -78 °C (150 mg,0.088 mmol) in THF (10 mL) was added a suspension of decamethyl ferrocenium triflate (84 mg, 0.17 mmol, 2.0 equiv.) in THF (4 mL). The solution was stirred at -78 °C for 30 minutes and then allowed to warm to room temperature and was stirred 2 h. All volatiles were subsequently removed from the dark brown solution and was triturated with hexanes (3 x 5 mL). The crude material was then washed with n-pentane (5 mL), followed by diethyl ether (10 mL) and then extracted with THF (7 mL) and filtered through a plug of Celite**.** The volatiles were subsequently removed from the extract to afford 87 mg (58% yield) of spectroscopically pure **4**. To obtain single-crystals suitable for X-Ray diffraction, complex **4** was dissolved in 1 mL of THF and transferred a 4 mL vial. This vial was then inserted into a 20 mL vial with 3 mL of hexamethyldisiloxane. The sealed vial was then left at -40 °C over the course of a week to afford single crystals of **4-HMDSO** suitable for X-Ray diffraction.^{1}H NMR (400 MHz, CD_3CN): δ 9.33 (broad s, 6H,

Ar-H, $W_{1/2}$= 24 Hz), 8.66 (broad s, 6H, Ar-*H*, $W_{1/2}$= 14 Hz), 2.33 (broad s, 54H, ^{t}Bu, $W_{1/2}$= 15 Hz), -0.23 (broad s, 54H, ^{t}Bu, $W_{1/2}$= 35Hz), -37.1 (broad s, 30H, $[Cp^*_2Fc]^+$, $W_{1/2}$= 520 Hz).

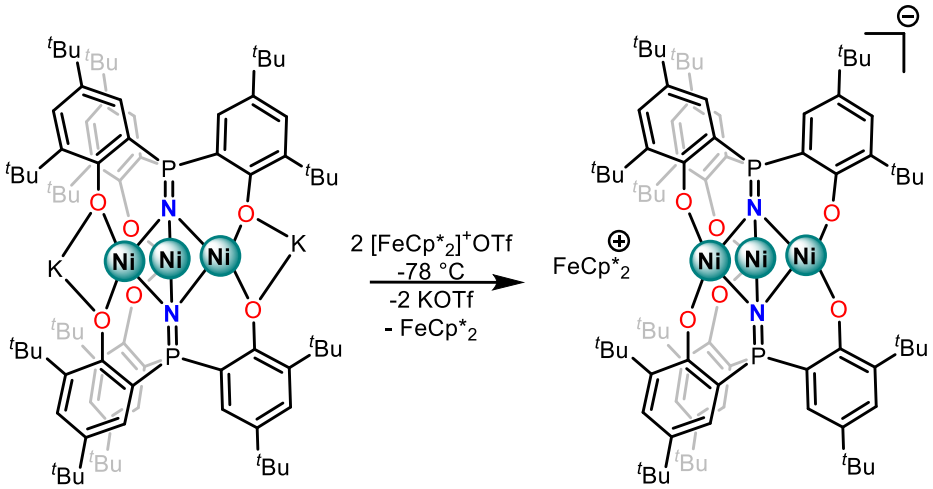

2[K] $[(O_3PN)_2Ni_3]$DME
3-DME

$[FeCp^*_2]^+[(O_3PN)_2Ni_3]^-$
4

Evans Method for 4: A solution of **4** with a concentration of 4.56 mmol/L (accounting for the presence of KOTf) in CD_3CN was prepared and transferred to an NMR tube. A sealed capillary of CD_3CN was subsequently added to the same NMR tube and was sealed. A ^{1}H NMR spectrum of this sample was collected on a 400 MHz spectrometer and a separation of 15.1 Hz was measured between the CD_2HCN signal inside the sealed capillary tube and inside the solution of **4**. Using this measured value and accounting for the diamagnetic susceptibility of **4** (-0.00126 emu/mol)[4], an effective magnetic moment of 2.80 Bohr magnetons was calculated. This value corresponds to two unpaired electrons, one assigned to the decamethyl ferrocenium cation and one to the anion.

NMR Characterization

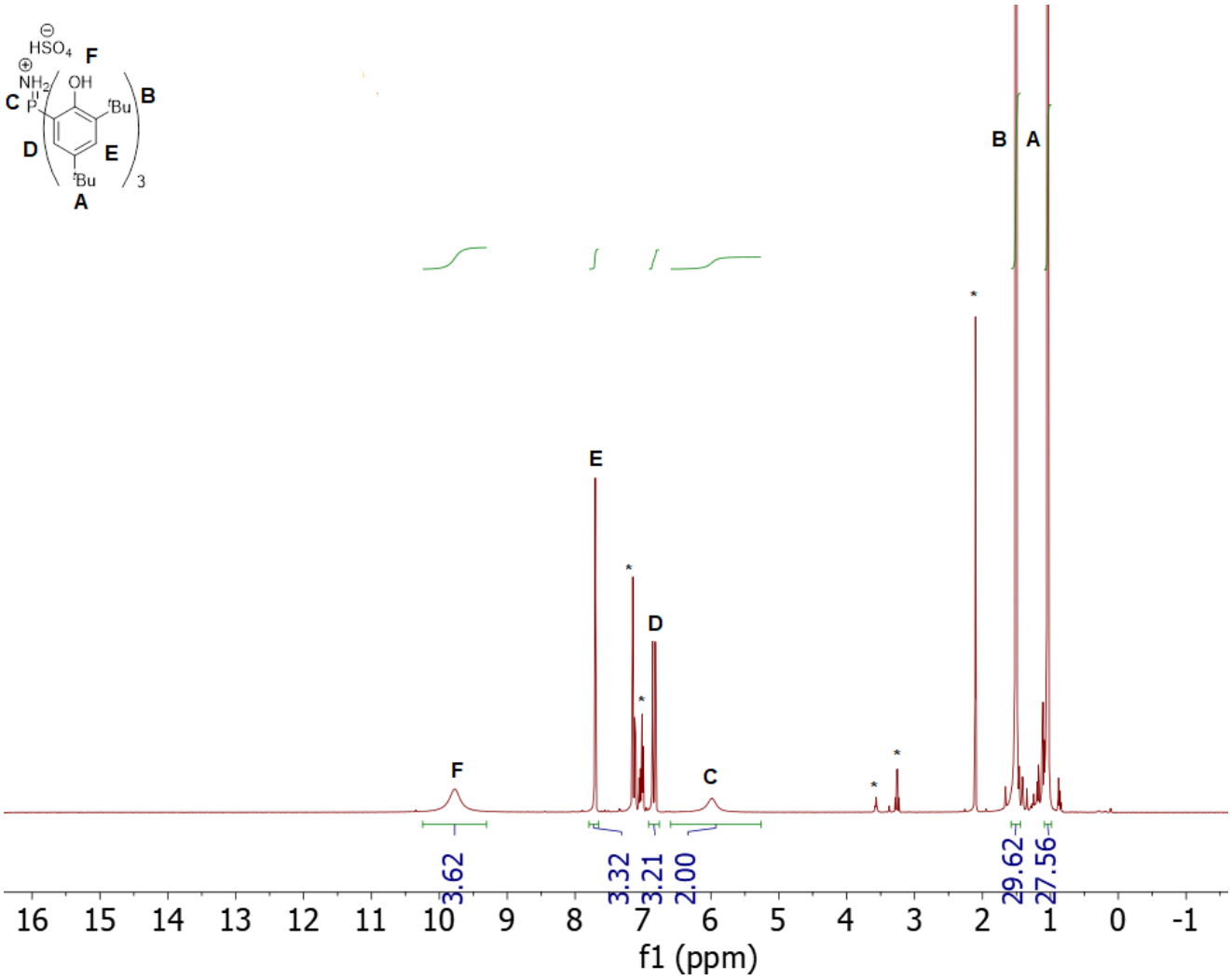

Figure S1: ^{1}H NMR spectrum of **2** (400 MHz, C_6D_6) * denotes residual diethyl ether, THF, and toluene

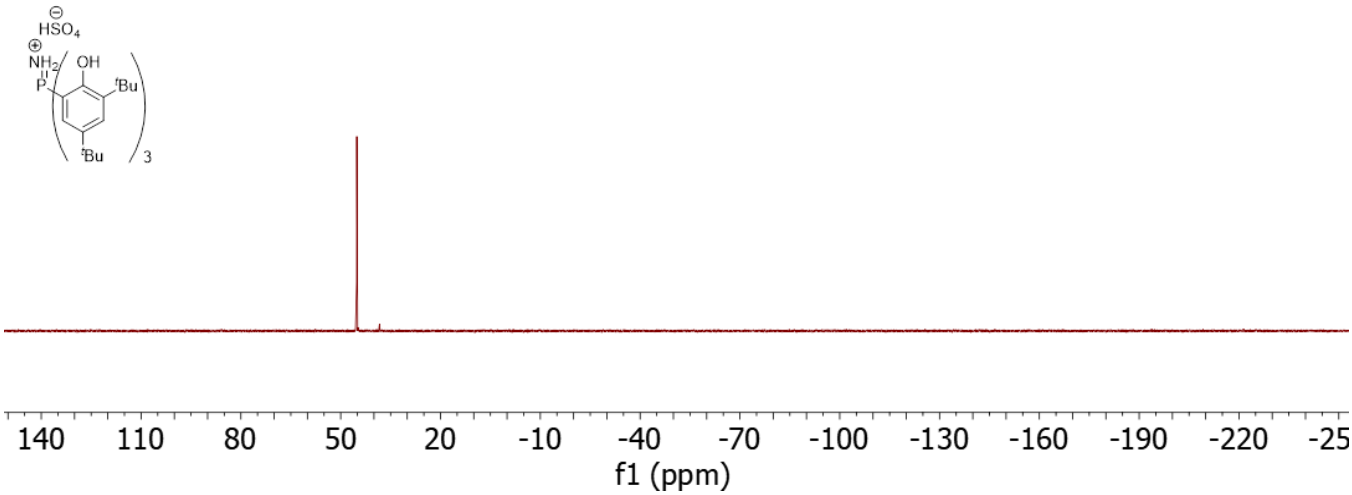

Figure S2: $^{31}P\{^{1}H\}$ NMR spectrum of **2** (121 MHz, C_6D_6)

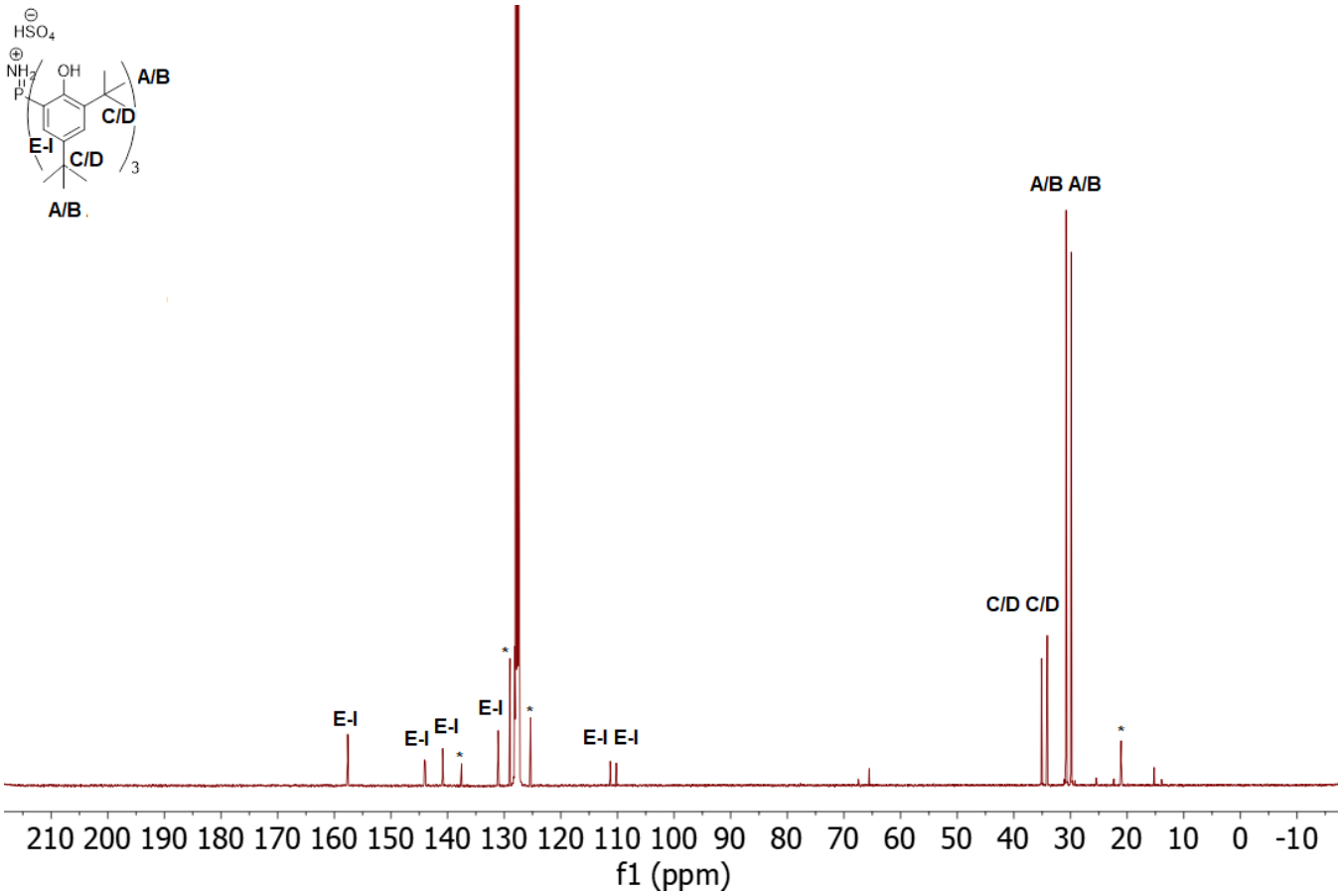

Figure S3: $^{13}C\{^{1}H\}$ NMR spectrum of **2** (101 MHz, C_6D_6) * denotes residual toluene

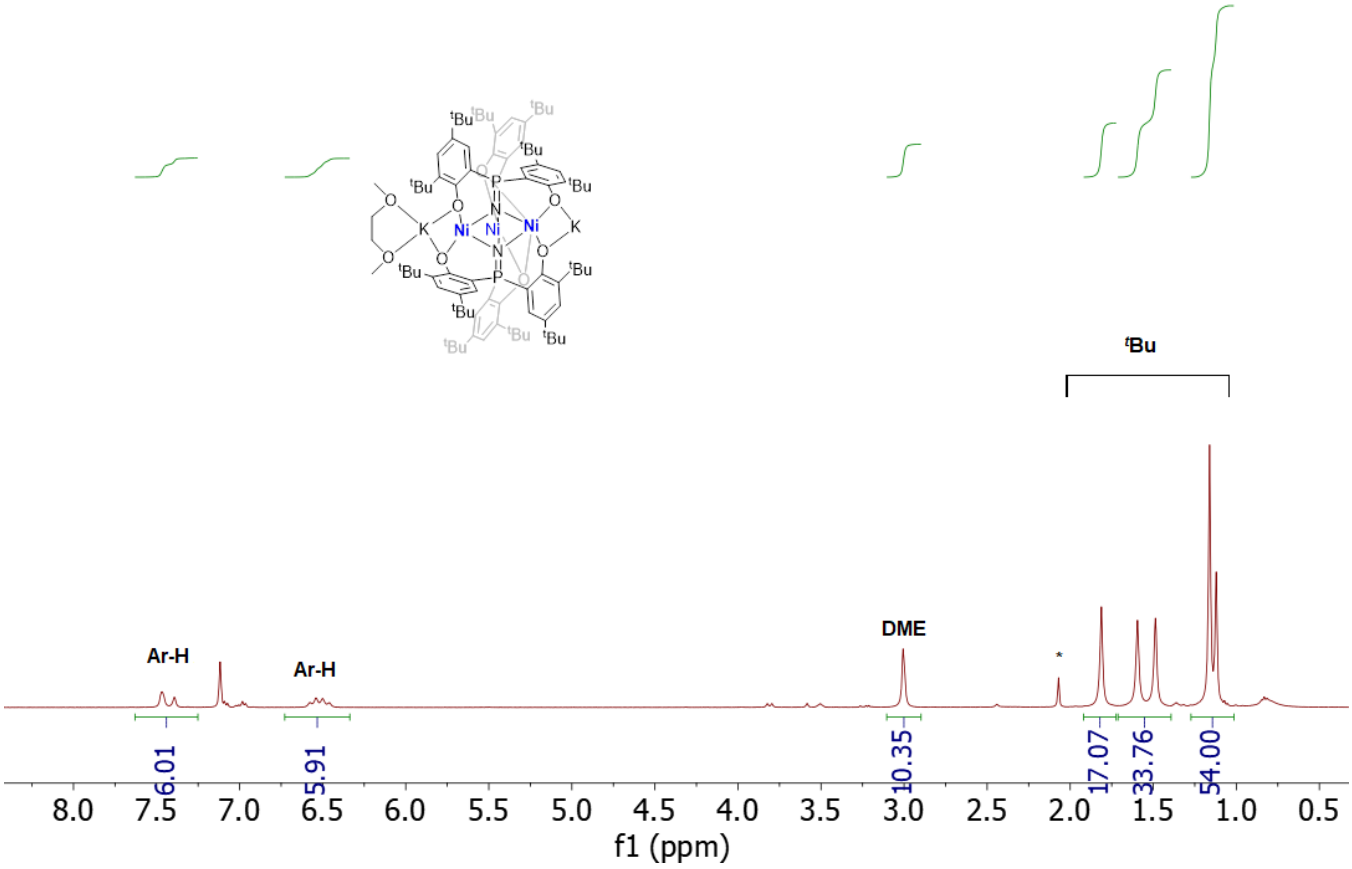

Figure S4:[1]H NMR spectrum of **3-DME** (400 MHz, C_6D_6) * denotes residual toluene

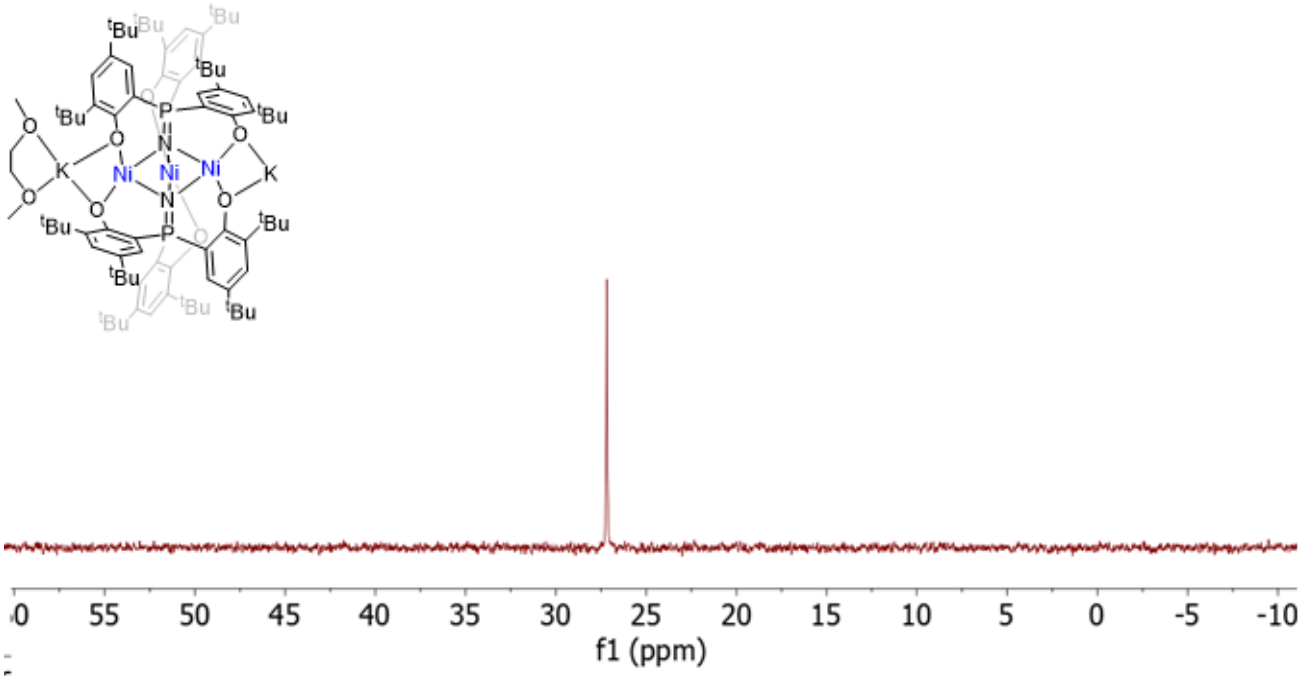

Figure S5:[31]P{[1]H} NMR spectrum of **3-DME** (121 MHz, C_6D_6)

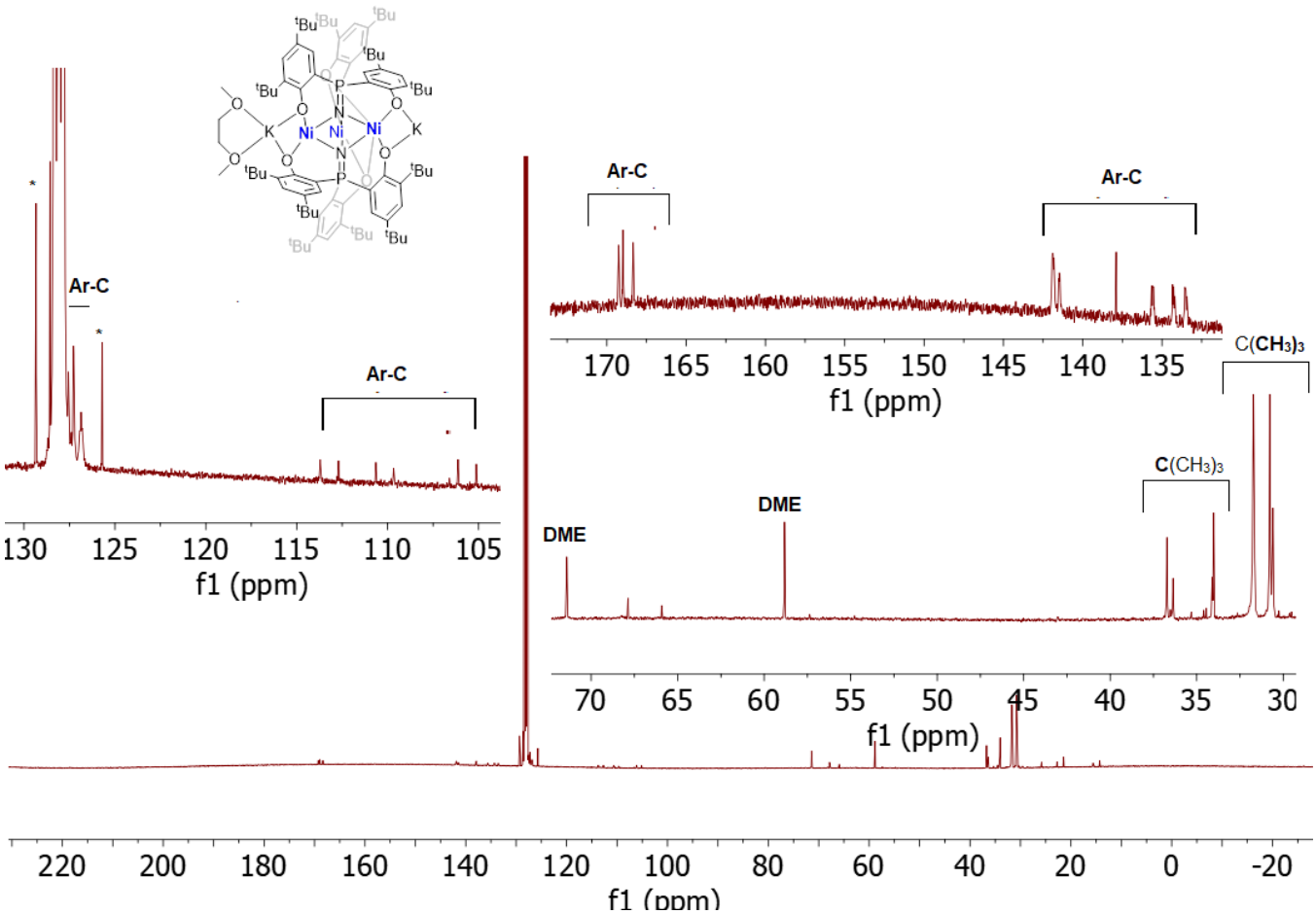

Figure S6:$^{13}C\{^{1}H\}$ NMR spectrum of **3-DME** (101 MHz, C_6D_6) * denotes residual toluene

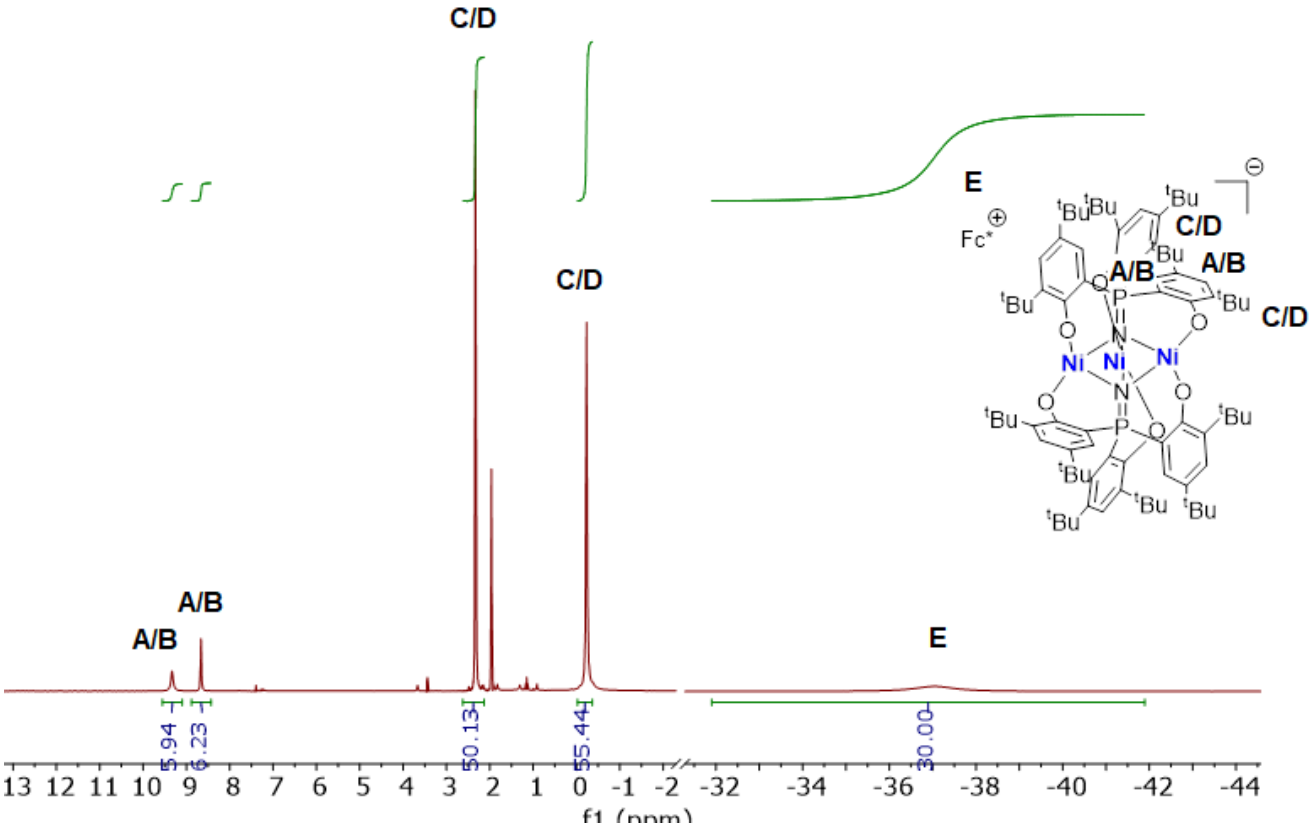

Figure S7:[1]H NMR spectrum of **4** (400 MHz, CD_3CN)

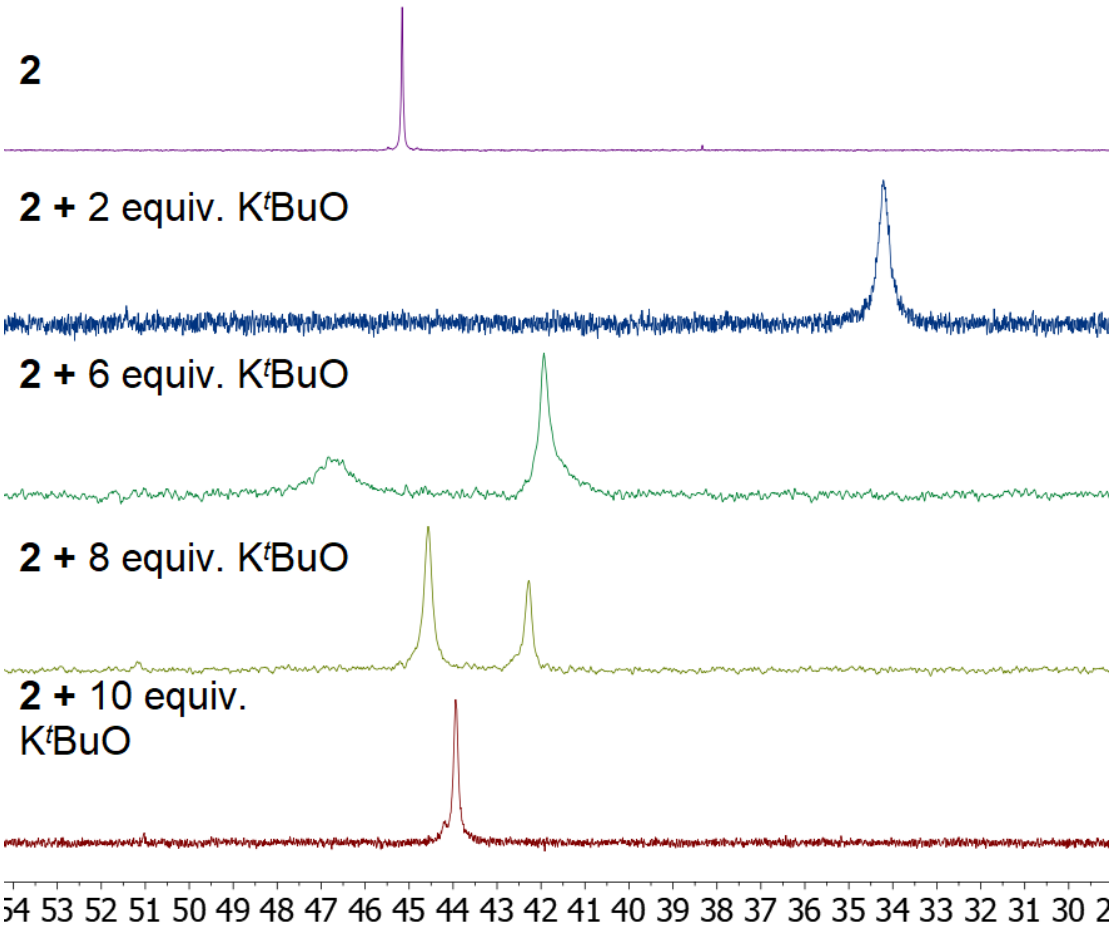

Figure S8: $^{31}P\{^{1}H\}$ NMR spectrum of **2** with varying amounts of K^{t}BuO (400 MHz, C_6D_6)

Cyclic Voltammetry Studies

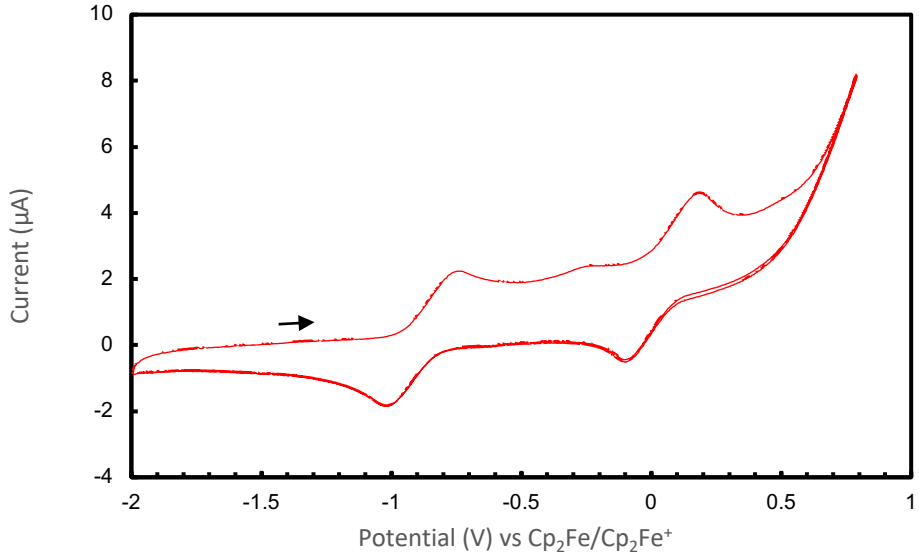

Figure S9: Cyclic voltammogram of **3-DME** in THF (0.1 M [^{n}Bu$_4$N]PF$_6$) scanned at 250 mV/s

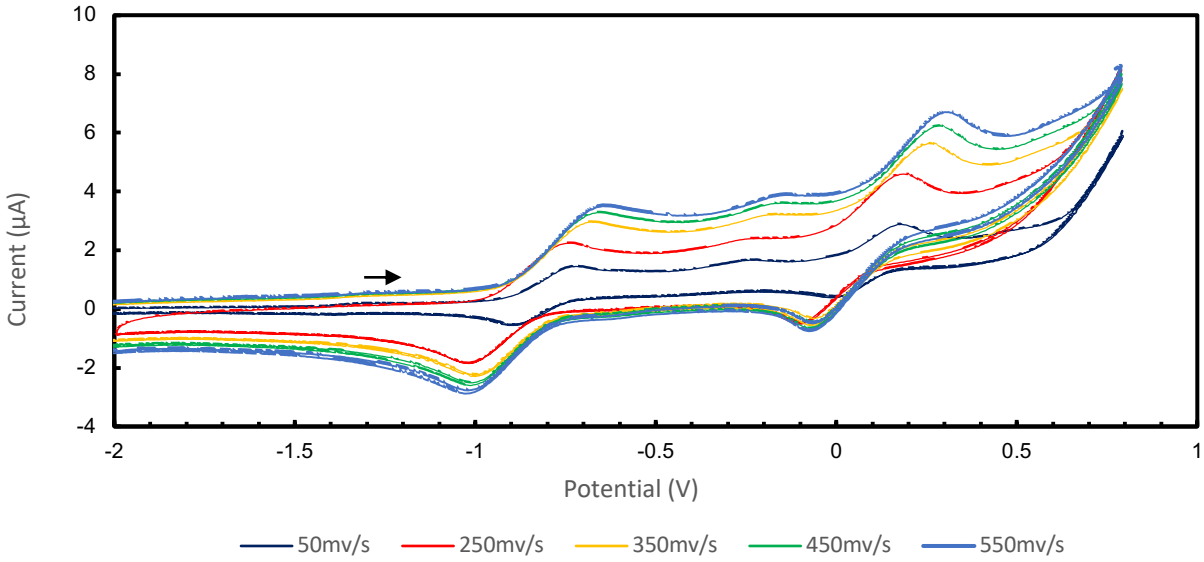

Figure S10: Scan rate dependence of the cyclic voltammogram of **3-DME** in THF (0.1 M [^{n}Bu$_4$N]PF$_6$)

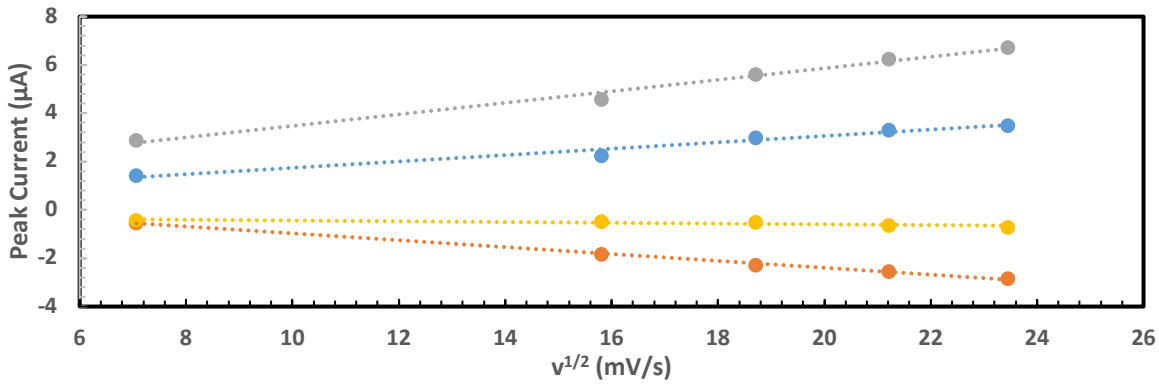

Figure S11: Scan rate dependence of the peak currents from the CV of **3-DME** in THF (0.1 M [^{n}Bu$_4$N]PF$_6$)

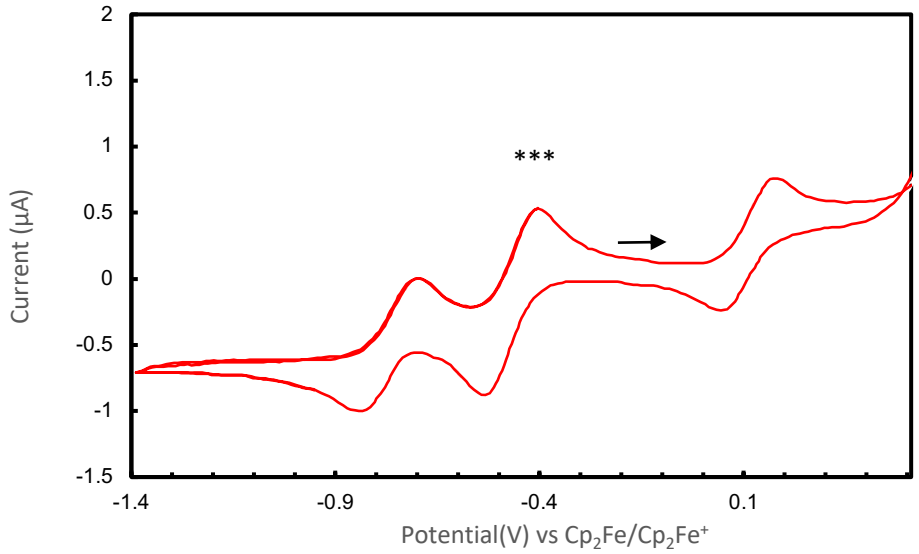

Figure S12: Cyclic voltammogram of **4** THF (0.1 M [^{n}Bu$_4$N]PF$_6$) scanned at 25 mV/s ***Redox couple for Cp*$_2$Fe$^+$/Cp*$_2$Fe

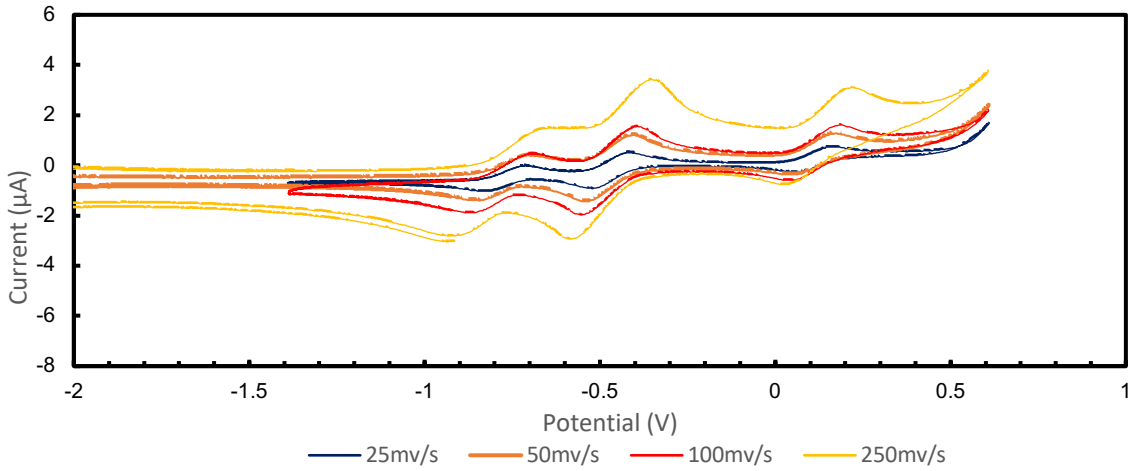

Figure S13: Scan rate dependence of the cyclic voltammogram of **4** in THF (0.1 M [^{n}Bu$_4$N]PF$_6$)

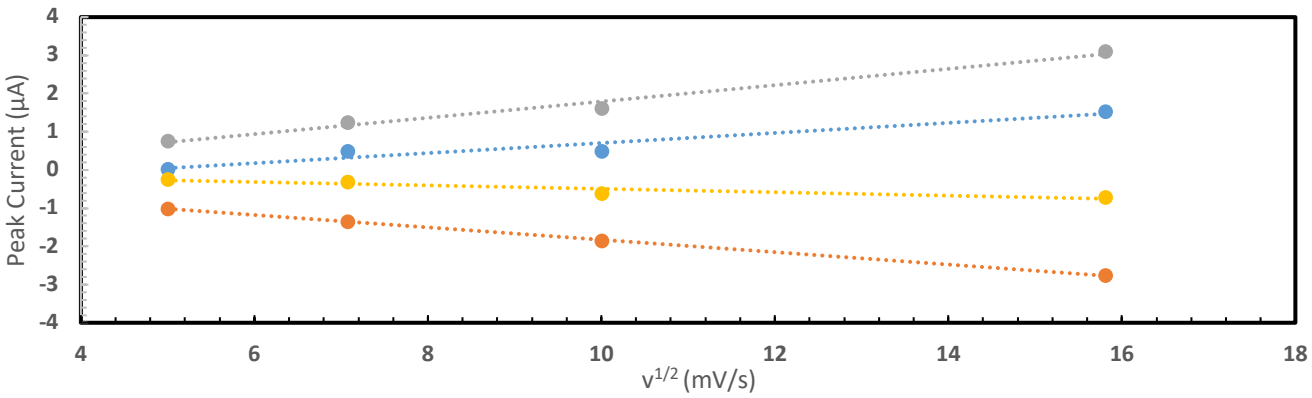

Figure S14: Scan rate dependence of the peak currents from the CV of **4** in THF (0.1 M [^{n}Bu$_4$N]PF$_6$)

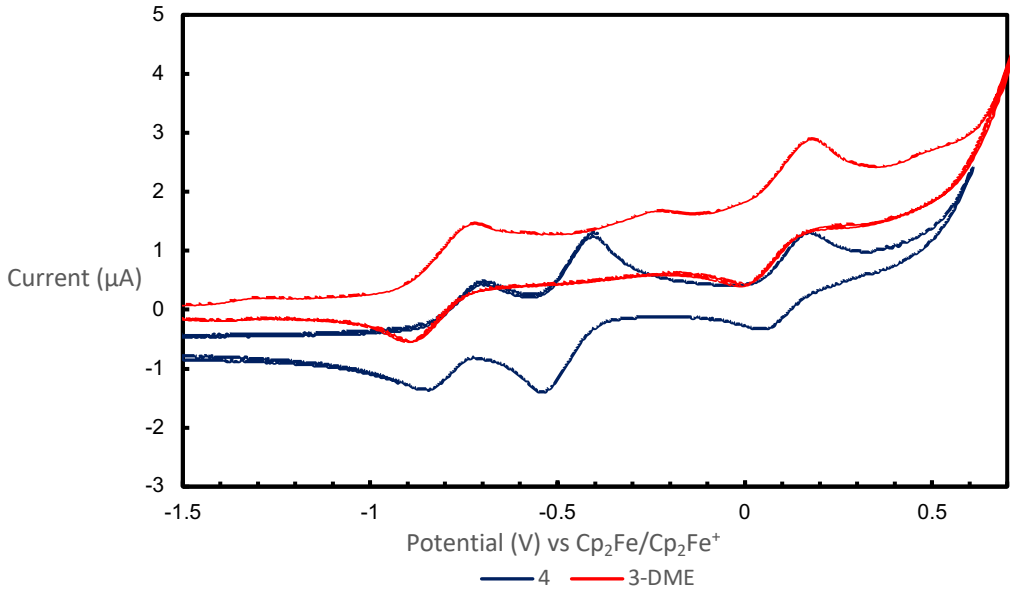

Figure S15: Cyclic voltammogram of **3-DME** and **4** THF (0.1 M [^{n}Bu$_4$N]PF$_6$) scanned at 50 mV/s

Crystallographic Information

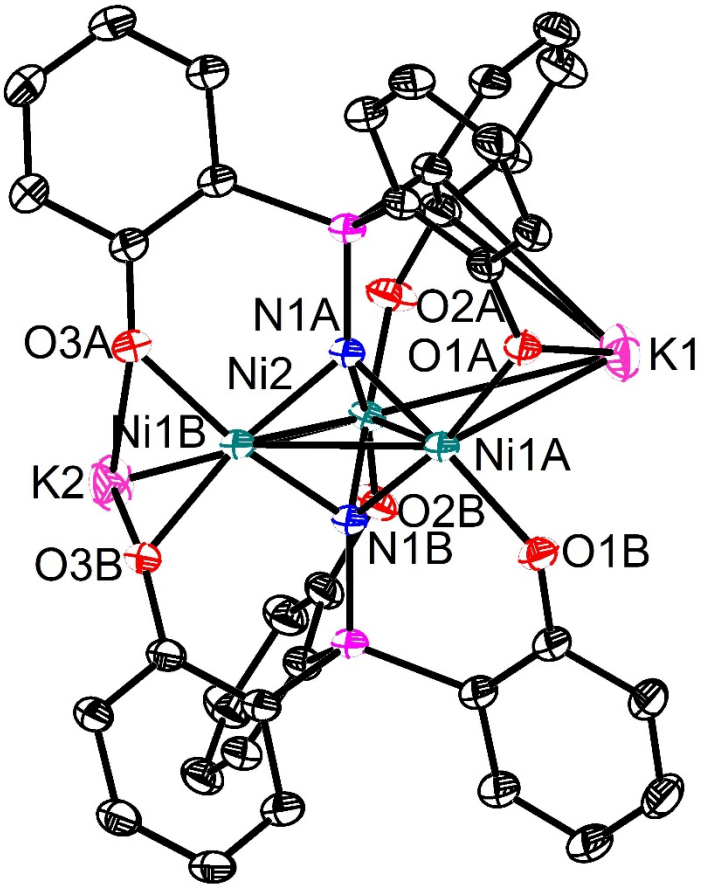

Figure S16: Solid-State structure of **3.** Ellipsoids are shown at the 50% probability level. Carbon atoms of tert-butyl groups, hydrogen atoms, and solvent molecules are excluded for clarity.

Special Refinement Details for 3: Crystallizes in a $C_{2/C}$ space group with half of the molecule in the asymmetric unit. The K center is modelled with 2 site disorder with occupancies of 0.80 and 0.20. Disorder is also extended to the hexamethyldisiloxane(HMDSO) bound to the potassium. Some of the methyl carbons on the HMDSO were refined as isotropic to avoid a non-positive definite. Additional two site disorder is present on one of the *tert*-butyl groups and was modelled with occupancies of 0.62 to 0.38.

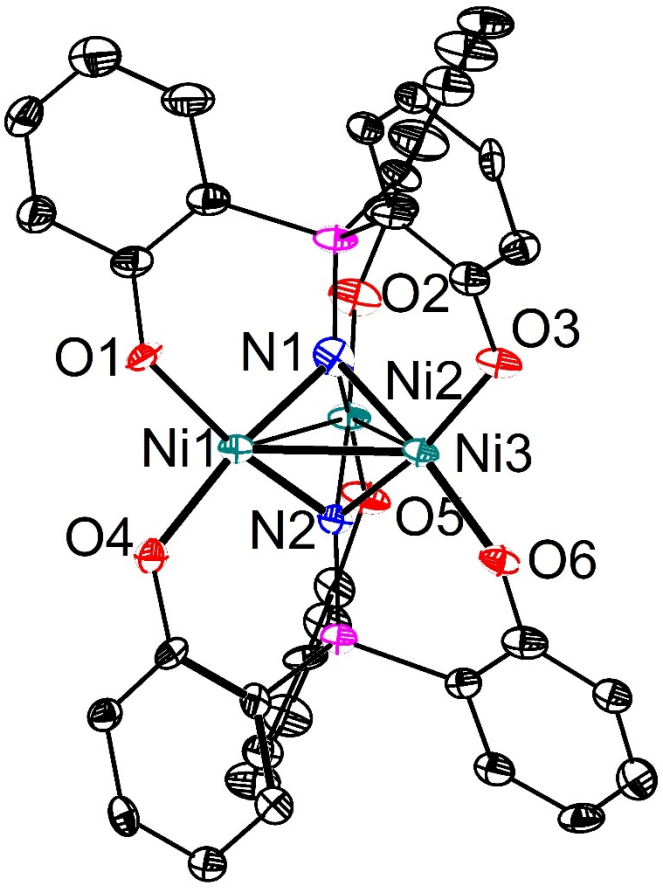

Figure S17: Solid-State structure of **4.** Ellipsoids are shown at the 50% probability level. Decamethyl ferrocenium, carbon atoms of tert-butyl groups, hydrogen atoms, and solvent molecules are excluded for clarity.

Special Refinement Details for 4: Crystallizes in a $P2_{1/C}$ space group with two outer-sphere HMDSO molecules. Two site disorder is present on one of the tert-butyl groups and was modelled with occupancies of 0.83 to 0.17. Additional disorder was present on another *tert*-butyl group as well as the methyl groups of the HMDSO molecules but could not be modelled. All disorder was modelled based on the modest intensity data collected on **4**. The solvent mask PLATON SQUEEZE was used to supress two sections of electron density likely corresponding to two highly disordered molecules of hexamethyldisiloxane. Each void was calculated to be near 300 electrons per unit cell, which would be close to one molecule of HMDSO per asymmetric unit (Z=4).

	3	**4**
CCDC	1985597	1985598
Empirical formula	$C_{93.64}H_{148.93}K_2N_2Ni_3O_8P_2Si_4$	$C_{112.83}H_{176.5}FeN_2Ni_3O_{7.47}P_2Si_{2.94}$
Formula weight	1859.40	2057.28
Temperature/K	100.0(2)	100.0(2)
Crystal system	monoclinic	monoclinic
Space group	C2/c	$P2_1/c$
a/Å	28.067(6)	25.101(9)
b/Å	20.574(4)	30.772(12)
c/Å	18.052(4)	18.538(7)
α/°	90	90
β/°	97.215(7)	100.85(3)
γ/°	90	90
Volume/$Å^3$	10341(4)	14063(9)
Z	4	4
$\rho_{calc}g/cm^3$	1.194	0.972
μ/mm^{-1}	0.748	0.587
F(000)	3987.0	4434.0
Crystal size/mm^3	0.24 × 0.16 × 0.12	0.2 × 0.15 × 0.15
Radiation	MoKα (λ = 0.71073)	MoKα (λ = 0.71073)
2Θ range for data collection/°	4.566 to 58.486	3.12 to 55.146
Index ranges	$-38 \leq h \leq 38$, $-28 \leq k \leq 28$, $-24 \leq l \leq 24$	$-24 \leq h \leq 31$, $-36 \leq k \leq 39$, $-19 \leq l \leq 2$
Reflections collected	107191	164629
Independent reflections	14000 [R_{int} = 0.0627, R_{sigma} = 0.0395]	26796 [R_{int} = 0.0887, R_{sigma} = 0.0987]
Data/restraints/parameters	14000/0/620	26796/75/1313
Goodness-of-fit on F^2	1.122	1.133
Final R indexes [I>=2σ (I)]	R_1 = 0.0596, wR_2 = 0.1604	R_1 = 0.1339, wR_2 = 0.2709
Final R indexes [all data]	R_1 = 0.0882, wR_2 = 0.1884	R_1 = 0.1716, wR_2 = 0.2870
Largest diff. peak/hole / e $Å^{-3}$	1.20/-0.56	1.26/-1.37

Table S1: Crystal and refinement data for complexes **3** and **4**

Computational Details

General Considerations: All calculations were performed with DFT as implemented in ORCA program version 4.1.2. Geometry optimizations and electronic structure calculations were performed BP86 functionals were used with relativistic approximation ZORA.14 The def2-SVP basis set was used for C and H atoms while the def2-TZVP basis set was used for P, N, O, and Ni atoms.[6] All optimizations were performed ignoring molecular symmetry—crystallographic coordinates were used as a starting point. Energetic minima were confirmed with subsequent frequency calculations which did not return imaginary frequencies. Structures optimized in this manner showed good agreement with bond lengths and angles determined via single crystal X-ray diffraction (Table S2 and S3).

	3-Exp	**3-Calc**
Ni(1)-Ni(3)	2.6546(9) Å	2.6644 Å
Ni(1)-Ni(2)	2.5744(7) Å	2.5346 Å
Ni(2)-Ni(3)	2.5744(7) Å	2.5351 Å
Ni-N(range)	1.852(2)-1.865(2) Å	1.842-1.868 Å
Ni-O(range)	1.880(2)-1.892(2) Å	1.886-1.920 Å
N-Ni-N (range)	71.7(1)-72.2(7) °	72.298-73.296 °
O-Ni-O (range)	91.81(9)-92.34(9) °	90.574-91.004 °

Table S2: Comparison of Experimental and Calculated Structural Metrics of **3**

	4-Exp	**4-Calc**
Ni(1)-Ni(3)	2.477(2) Å	2.460 Å
Ni(1)-Ni(2)	2.636(2) Å	2.624 Å
Ni(2)-Ni(3)	2.657(2) Å	2.625 Å
Ni-N(range)	1.854(7)-1.869(7) Å	1.850-1.856 Å
Ni-O(range)	1.859(6)-1.890(6) Å	1.873-1.881 Å
N-Ni-N (range)	72.5(3)-73.0(3) °	73.369-73.534 °
O-Ni-O (range)	92.0(2)-92.6(3) °	89.058-89.536 °

Table S3: Comparison of Experimental and Calculated Structural Metrics of **4**

Atom	**Calculated Mulliken Spin Density (e^-)**
Ni(1)	0.387
Ni(2)	0.072
Ni(3)	0.389

Table S4: Computed Mulliken Spin Densities of **4**

Bond	**Löwdin Bond Order**
Ni(1)-Ni(3)	0.4287
Ni(2)-Ni(3)	0.3071
Ni(1)-Ni(2)	0.3070

Table S5: Löwdin Bond Orders of **4**

Qualitative bonding analysis

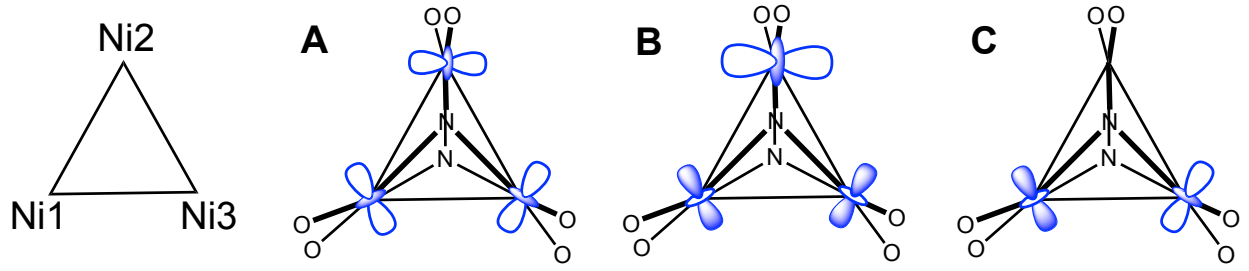

Figure S18. Qualitative MO representations of Ni-Ni interactions involving d_{z2} orbitals. MOs A-C are all occupied in **3**. C is only partially occupied in **4**, increasing the bond order between Ni1 and Ni3 by removing an electron from an antibonding interaction and promoting a shortening of the Ni1-Ni3 distance. This electronic structure localizes the spin on Ni1 and Ni3, primarily.

Orbital and Energy Relative to HOMO	Ni2 Ni1 Ni3	Ni1 Ni3 Ni2	Ni3 Ni2 Ni1
LUMO +2.670 eV	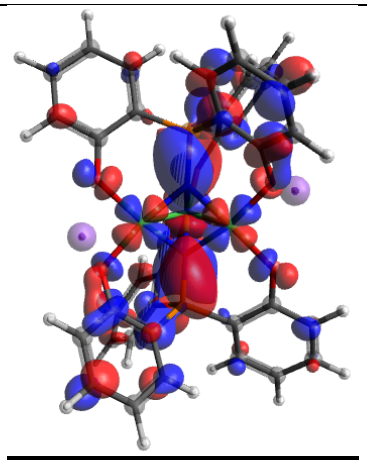	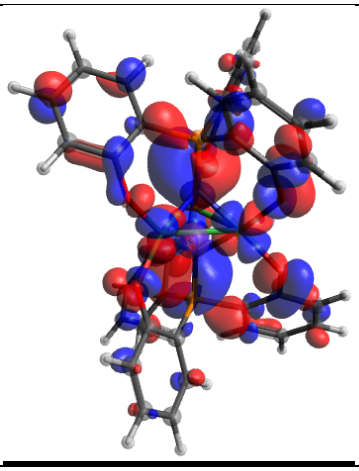	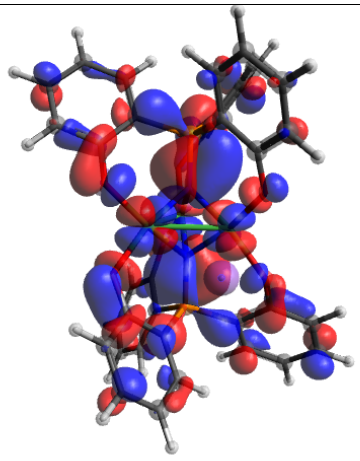

HOMO 0.000 eV	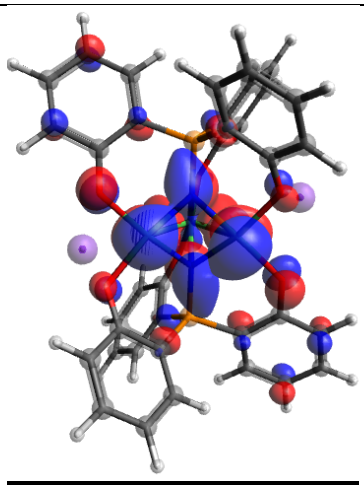	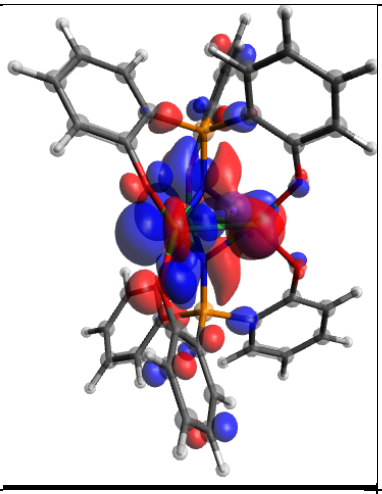	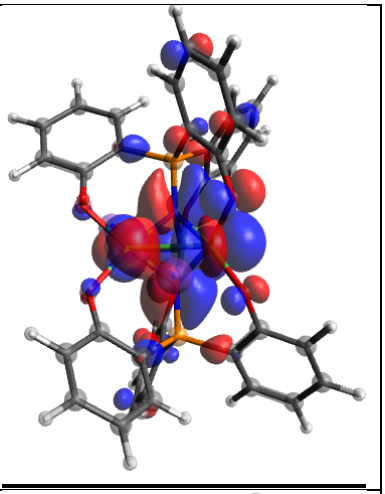
HOMO-1 -0.073 eV	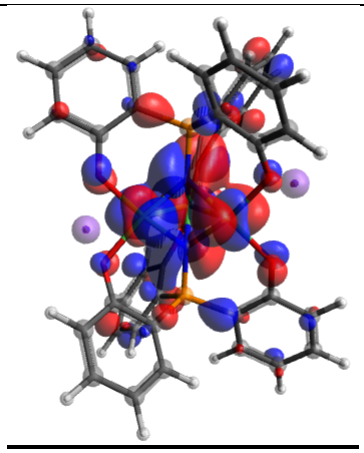	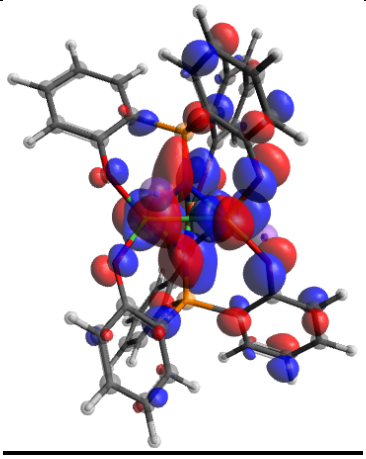	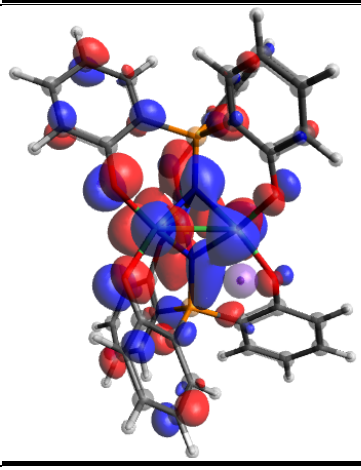
HOMO-2 -0.219 eV	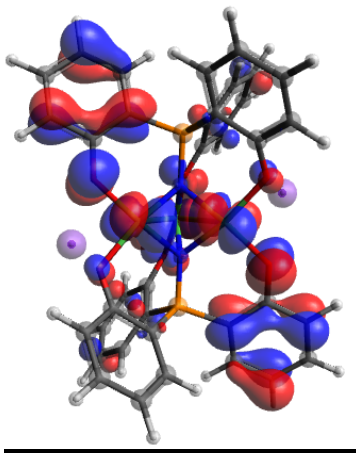	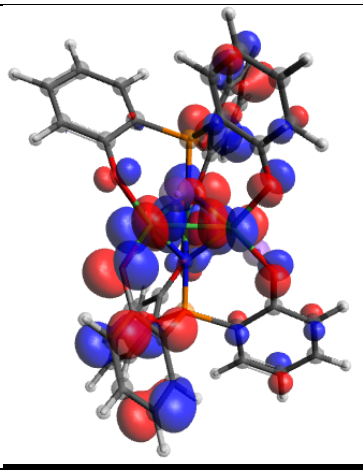	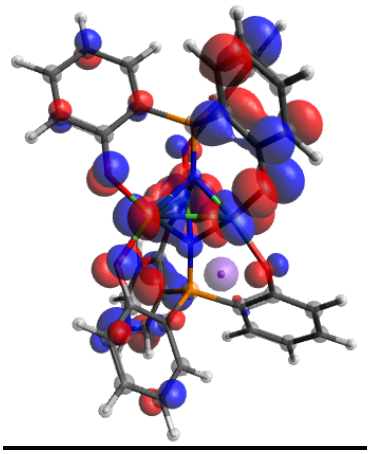

HOMO-3 -0.448 eV	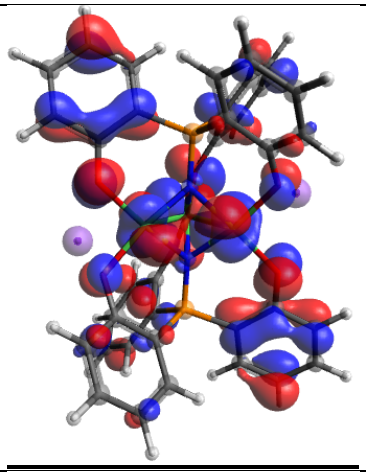	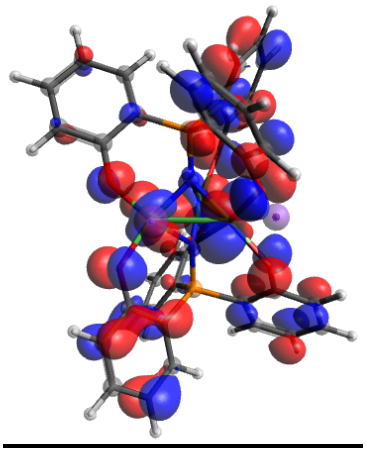	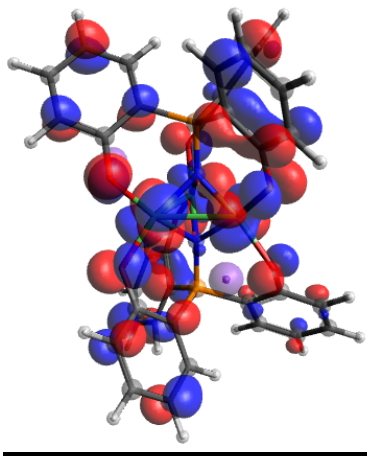
HOMO-4 -0.532 eV	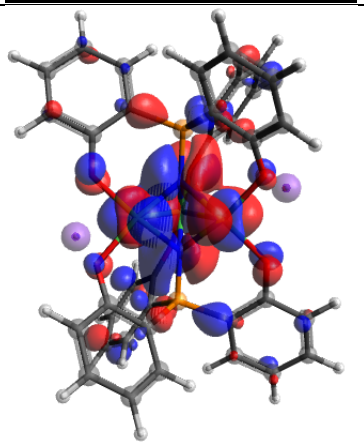	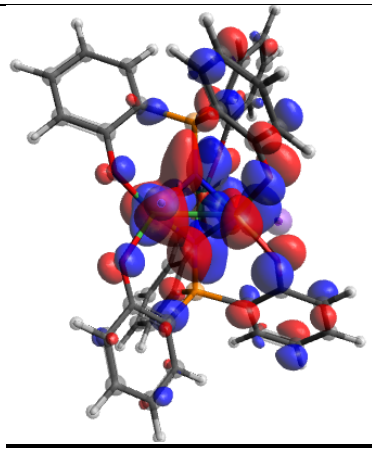	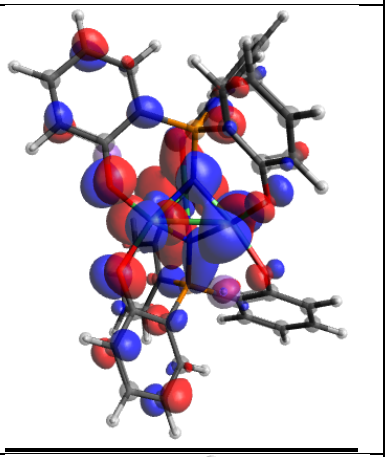
HOMO-5 -0.537 eV	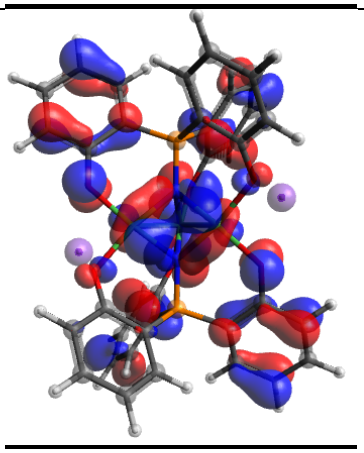	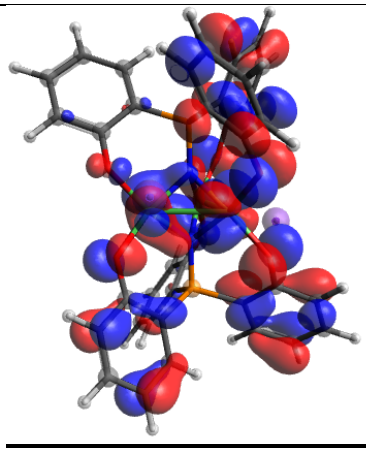	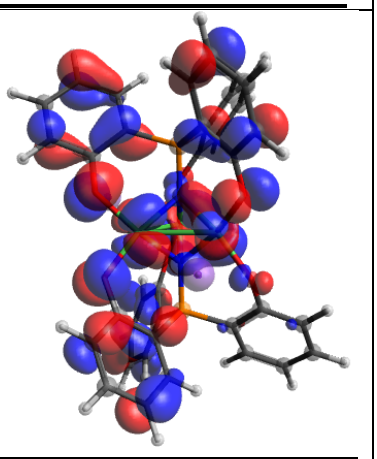

HOMO-6 -0.674 eV	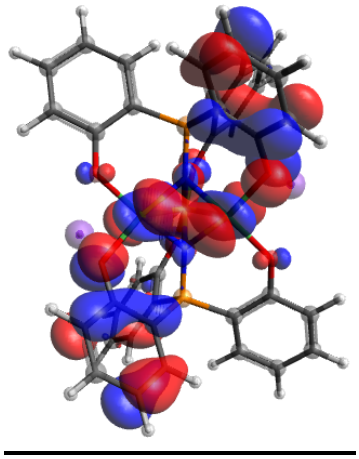	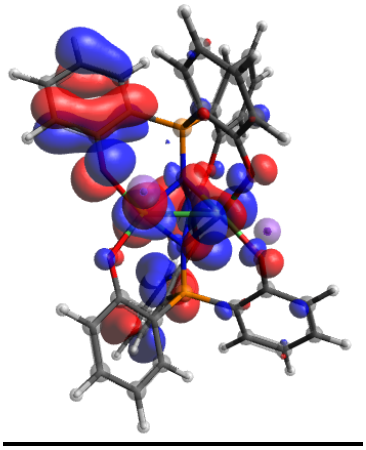	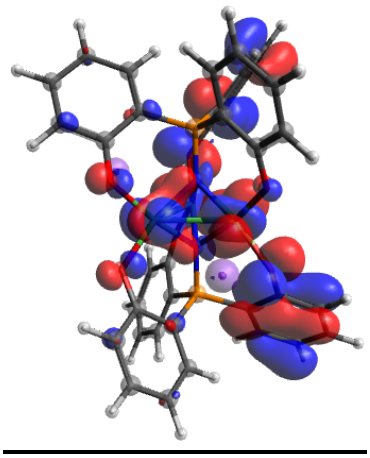
HOMO-7 -0.926 eV	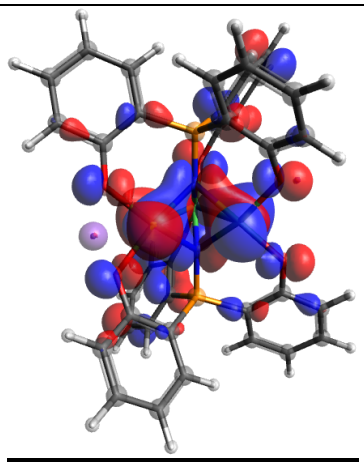	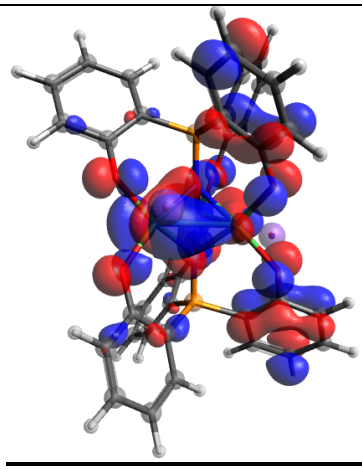	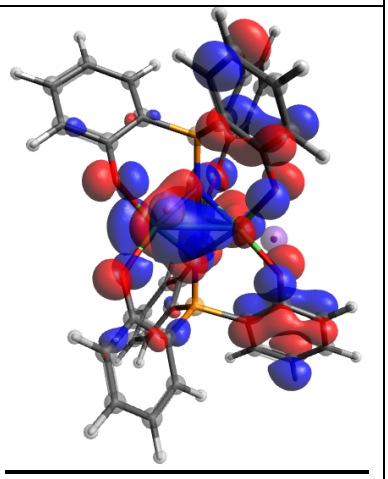
HOMO-8 -1.099 eV	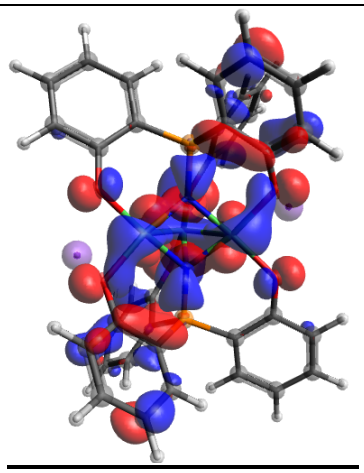	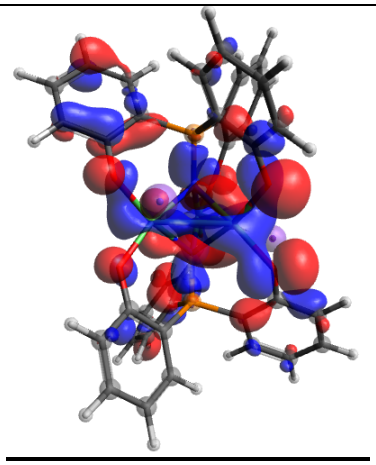	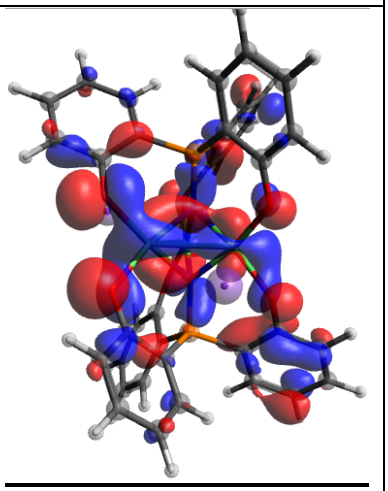

HOMO-9 -1.191 eV	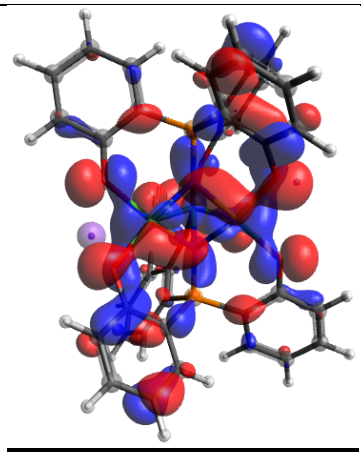	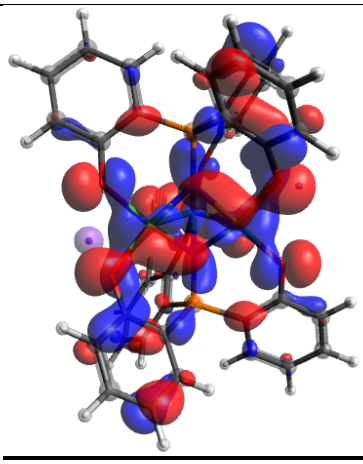	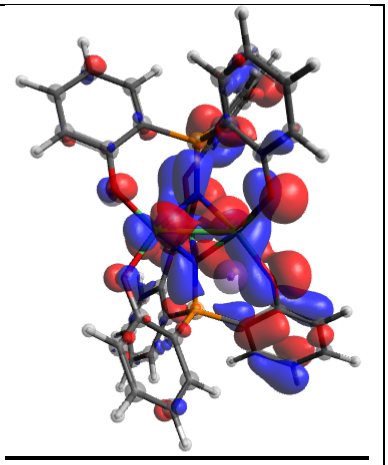
HOMO-10 -1.238 eV	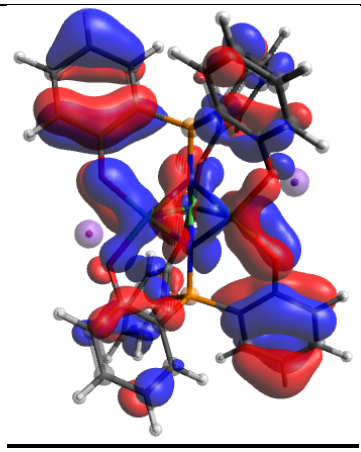	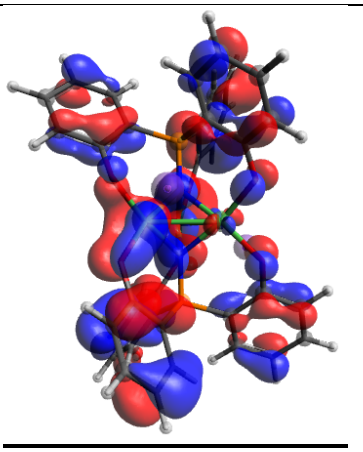	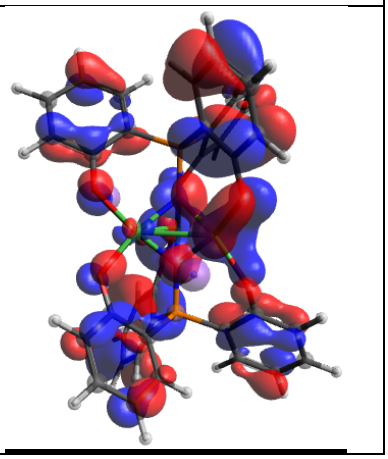

Table S6. Molecular Orbitals of 3

Orbital and Energy Relative to SOMO	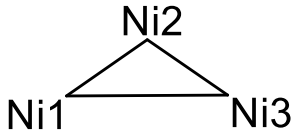	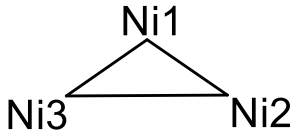	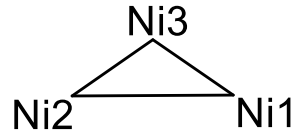
LUMO +2.495 eV	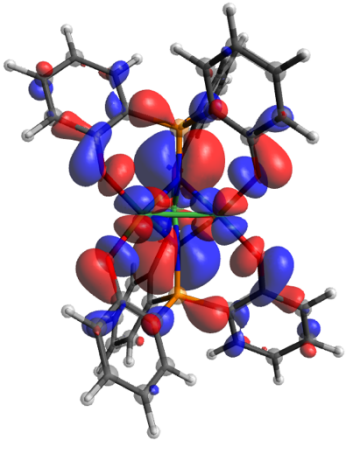	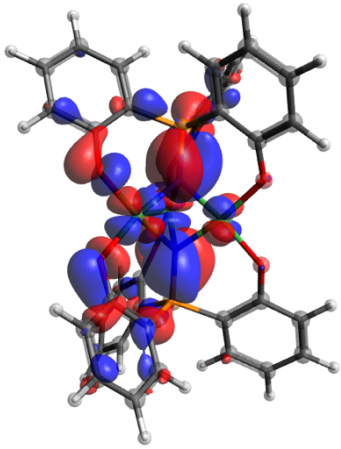	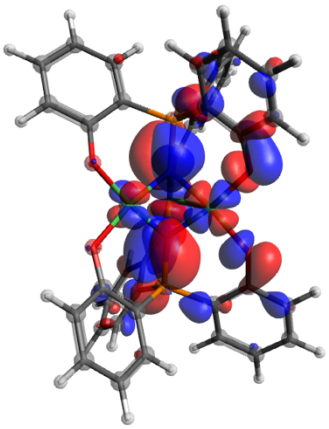

SOMO 0.000 eV	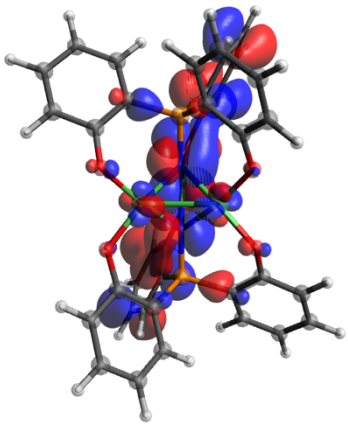	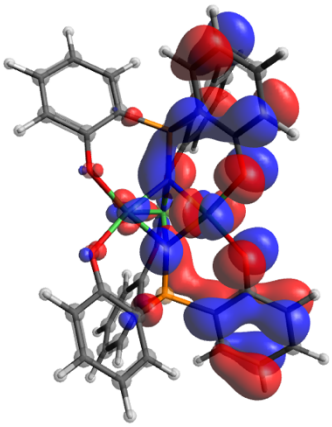	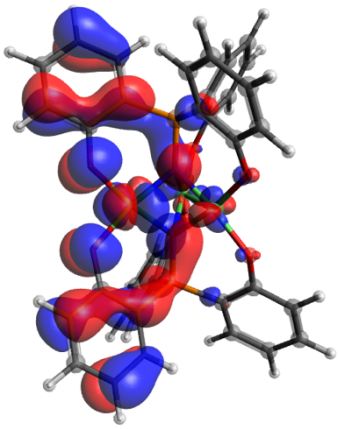
SOMO-1 -0.049 eV	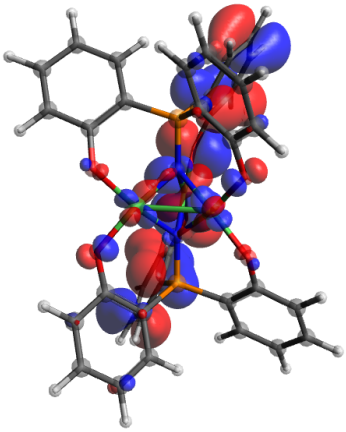	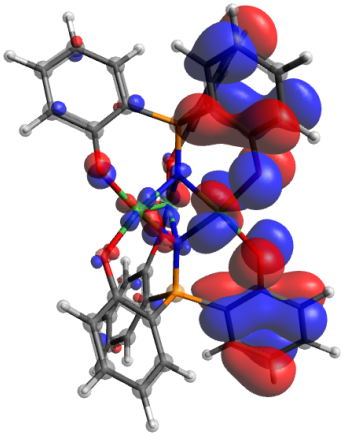	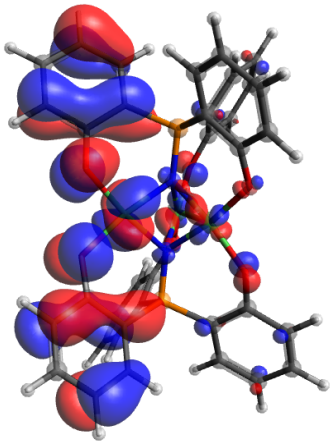
SOMO-2 -0.197 eV	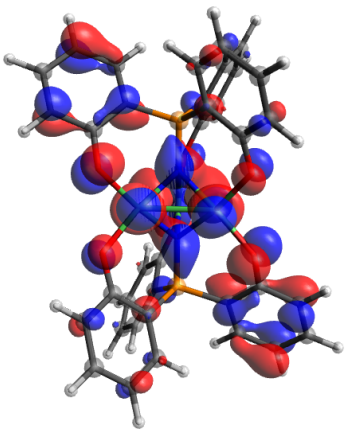	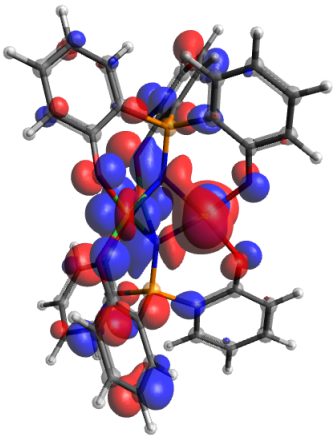	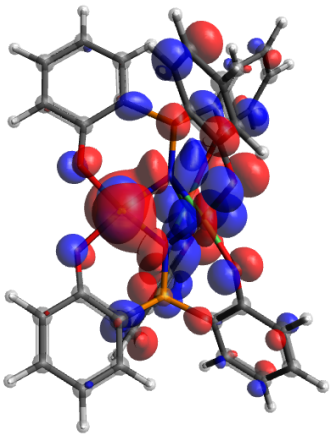
SOMO-3 -0.321 eV	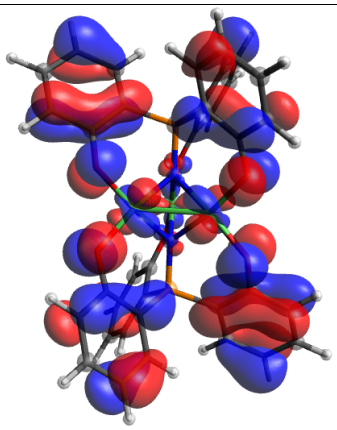	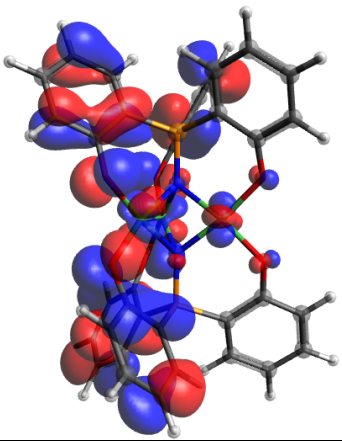	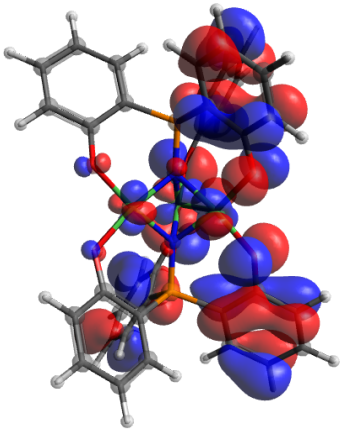

SOMO-4 -0.337 eV	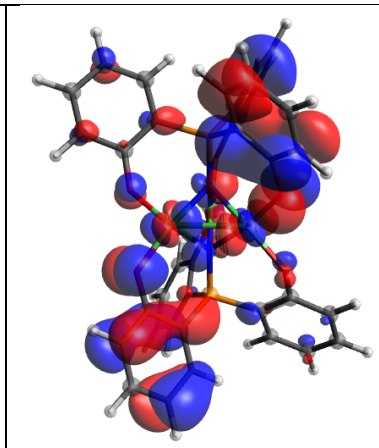	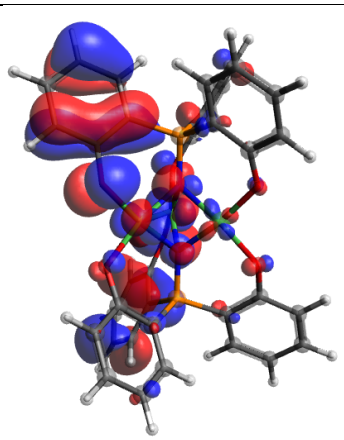	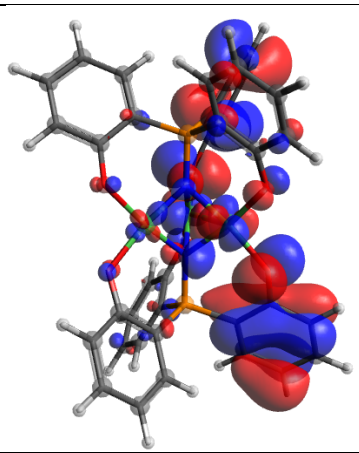
SOMO-5 -0.410 eV	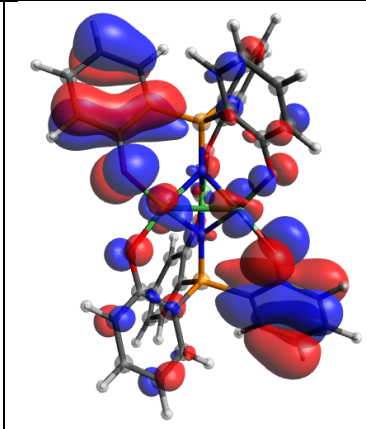	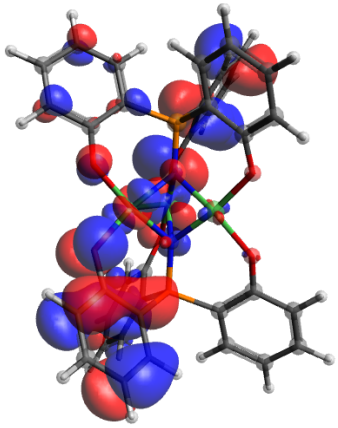	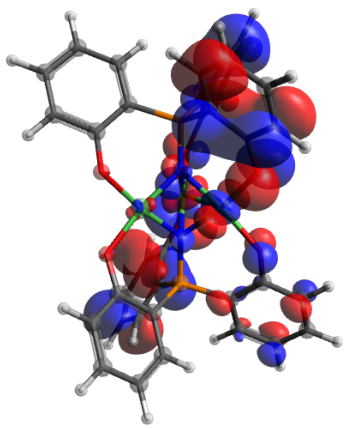
SOMO-6 -0.562 eV	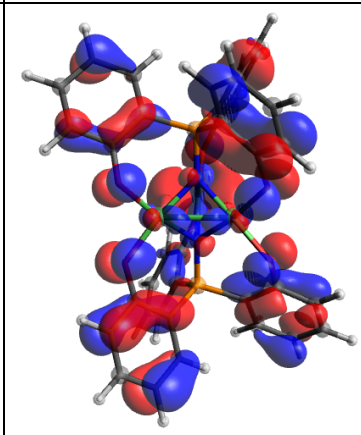	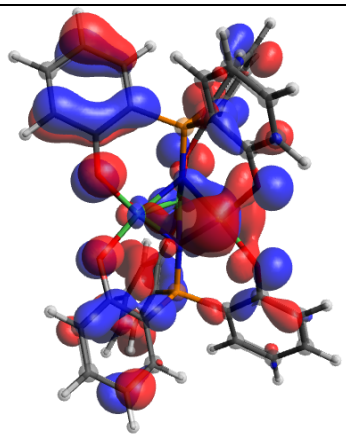	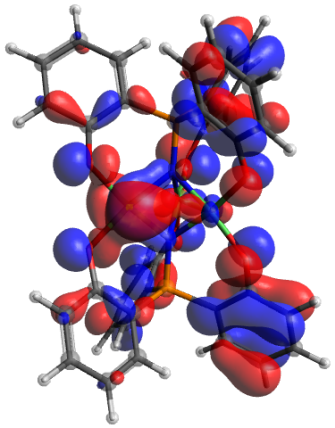
SOMO-7 -0.908 eV	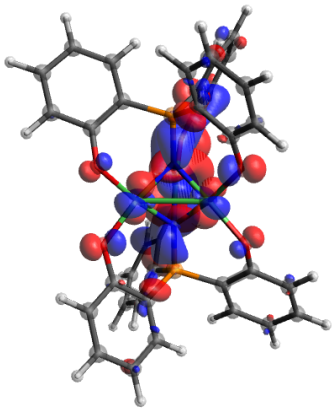	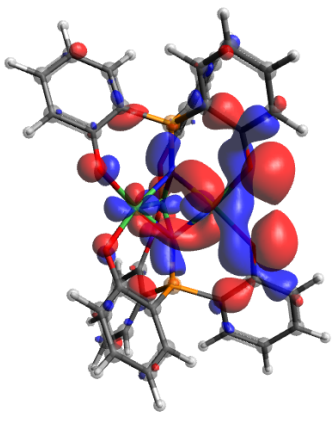	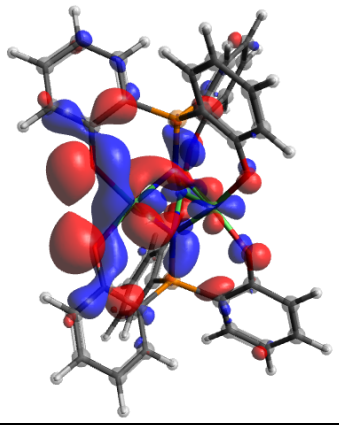

SOMO-8 -0.916 eV	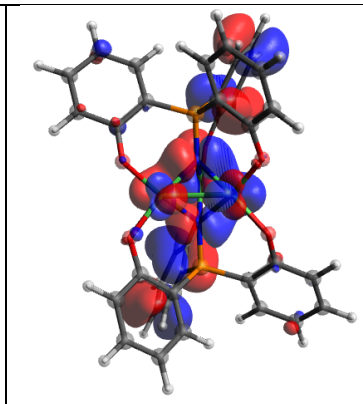	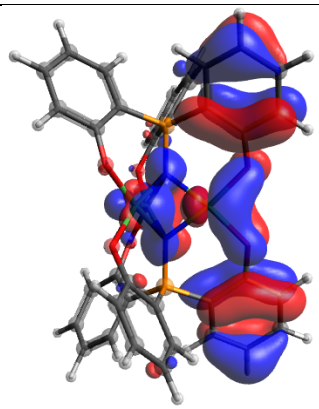	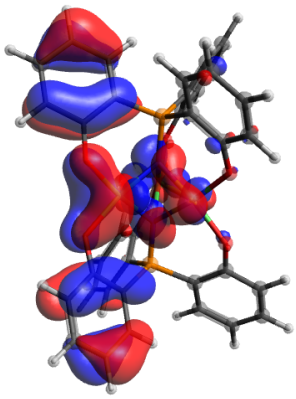
SOMO-9 -1.076 eV	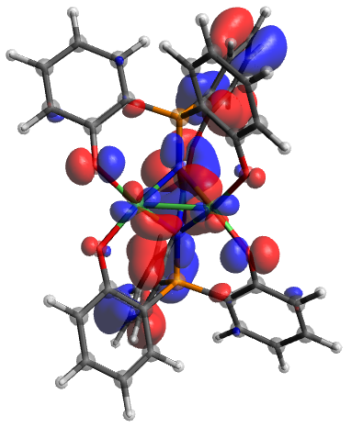	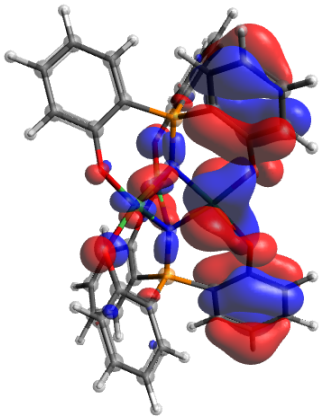	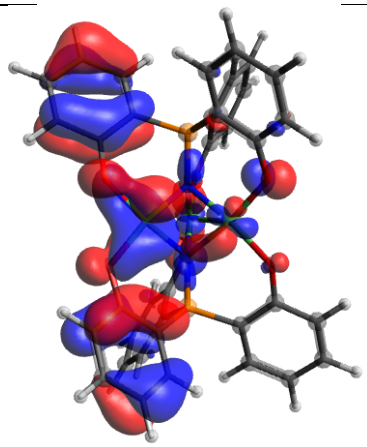
SOMO-10 -1.148 eV	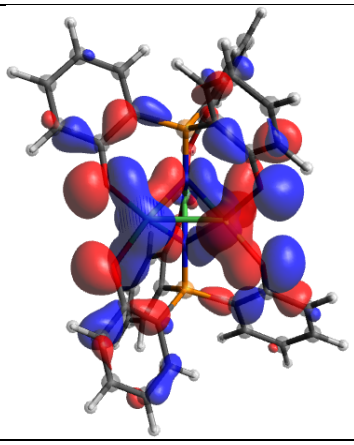	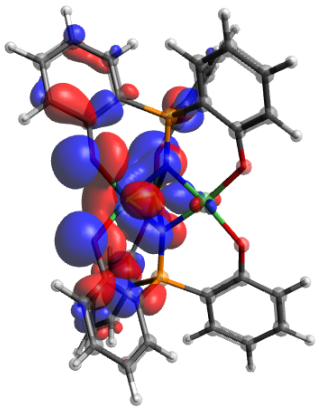	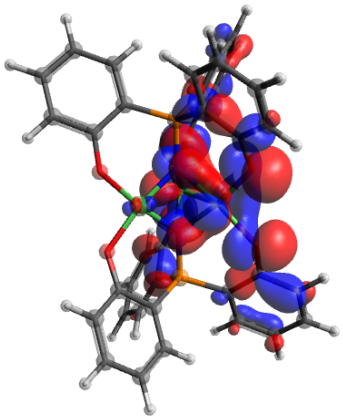

Table S7. Molecular Orbitals of 4

Cartesian Coordinates for 3

Ni	14.83015	3.89440	4.61857	P	13.74982	4.53891	1.75600
Ni	13.50475	6.05100	4.48003	O	13.34593	7.37706	3.14030
Ni	12.18008	3.89447	4.34227	O	16.33410	3.70010	3.49701
K	16.87227	5.71923	5.71246	O	11.14933	3.31762	2.82767
K	10.13878	5.71881	3.24712	O	13.66436	7.37688	5.82028
P	13.26014	4.53880	7.20463	O	10.67650	3.69919	5.46385

O	15.86097	3.31801	6.13304	C	12.92379	3.06878	1.14623
N	13.38509	4.54249	5.57595	C	11.00190	1.56628	1.23217
N	13.62506	4.54206	3.38468	C	17.85373	4.15574	1.76763
C	15.52437	7.01053	9.56821	C	12.85103	5.98180	1.16316
C	14.83493	5.91266	9.04366	C	13.43764	2.32761	0.05772
H	14.81746	4.96205	9.60042	H	14.40095	2.62662	-0.38474
C	14.26937	1.22676	9.41345	C	11.68904	2.68586	1.78384
C	14.18816	7.20294	7.01191	C	12.11391	8.31110	1.36570
C	14.08634	3.06882	7.81418	C	11.47234	8.21770	0.13042
C	16.00849	1.56675	7.72869	H	10.94362	9.09854	-0.26962
C	9.15629	4.15586	7.19249	C	11.51388	0.86058	0.13977
C	14.15897	5.98165	7.79762	H	10.95656	-0.00709	-0.24887
C	13.57231	2.32760	8.90260	C	16.50571	4.12634	2.25748
H	12.60880	2.62637	9.34475	C	15.48765	4.58519	1.33352
C	15.32125	2.68617	7.17676	C	17.17666	5.09643	-0.38055
C	14.89687	8.31062	7.59463	C	15.84943	5.07510	0.05158
C	15.53834	8.21730	8.82997	H	15.05689	5.45735	-0.61183
H	16.06737	9.09804	9.22980	C	18.17824	4.61898	0.49448
C	15.49644	0.86103	8.82103	H	19.23232	4.61590	0.17261
H	16.05378	-0.00659	9.20973	H	17.43337	5.47955	-1.37890
C	10.50447	4.12602	6.70308	H	18.63426	3.78194	2.44894
C	11.52235	4.58510	7.62713	H	16.03835	6.93533	10.53770
C	9.83299	5.09685	9.34067	H	14.91112	9.24602	7.01396
C	11.16032	5.07531	8.90889	H	13.86038	0.65328	10.25831
H	11.95277	5.45735	9.57250	H	16.94989	1.26385	7.24558
C	8.83155	4.61947	8.46544	H	8.37587	3.78212	6.51103
H	7.77738	4.61666	8.78706	H	9.57607	5.48028	10.33884
C	11.48589	7.01077	-0.60756	H	10.97170	6.93550	-1.57694
C	12.17503	5.91278	-0.08290	H	12.09991	9.24660	1.94620
H	12.19219	4.96206	-0.63948	H	13.14967	0.65314	-1.29782
C	12.74070	1.22663	-0.45296	H	10.06076	1.26312	1.71561
C	12.82215	7.20325	1.94863				

Cartesian Coordinates for 4

Ni	3.34534	19.20421	9.49577	C	2.33012	20.18487	12.00876
Ni	4.50849	16.85250	9.44126	C	3.28224	16.56126	12.59528
Ni	5.78023	19.11482	9.83451	C	3.43475	19.93585	14.22065
P	4.90609	18.59365	6.86610	H	4.18184	19.42948	14.85190
P	4.18064	18.08245	12.30425	C	1.56427	21.24325	12.59319
O	6.84382	19.49448	11.33742	C	6.56295	17.19919	5.13579
O	2.11626	19.91615	10.72916	H	6.74371	18.18343	4.67599
O	7.04196	20.00021	8.75663	C	3.27734	18.76485	6.13981
O	4.79662	15.64585	8.03755	C	2.67497	20.98152	14.75342
O	2.31142	19.92015	8.09813	C	1.83308	18.49120	4.17560
O	4.15972	15.41238	10.58737	C	6.00441	17.30323	14.24145
N	4.69682	18.43029	8.49191	H	5.17119	16.70515	14.64265
N	4.39019	18.22532	10.67665	C	8.12546	18.80573	13.18967
C	5.88995	20.06214	6.57249	C	1.80713	15.26281	14.06627
C	7.52375	22.26621	5.94309	C	3.44976	15.43460	11.70698
H	8.17061	23.12583	5.70457	C	7.15284	16.05861	4.58255
C	7.66280	21.63128	7.17767	C	2.45205	16.45973	13.74010
C	6.89181	18.79880	12.46616	H	2.31464	17.34456	14.38122
C	6.84745	20.51625	7.55212	C	5.81189	18.03512	13.04326
C	1.00378	19.65841	6.15623	C	6.12082	14.70491	6.33547
C	6.55335	21.83591	5.01065	C	6.91224	14.80634	5.19056
C	0.81270	19.19411	4.85367	H	7.36623	13.89520	4.76865
H	-0.15580	19.36849	4.35780	C	8.28679	18.09355	14.37939
C	5.51084	15.84975	6.93932	H	9.25964	18.12404	14.89599
C	1.72770	21.62439	13.92537	C	2.78416	14.22473	12.08186
H	1.11909	22.45060	14.32688	C	1.99250	14.14089	13.22803
C	5.74504	20.74285	5.33682	H	1.49484	13.18770	13.46903
H	4.97968	20.39983	4.62296	C	7.23020	17.32416	14.91473
C	3.26335	19.51038	12.87870	H	5.95267	13.73147	6.82132
C	2.23322	19.45512	6.85799	H	7.79435	16.14018	3.69282
C	3.05421	18.28423	4.82545	H	1.67301	18.10692	3.15750
H	3.85937	17.73471	4.31297	H	0.20079	20.18921	6.69044
C	5.73390	17.11707	6.28302	H	6.43030	22.35005	4.04612

H	8.40079	21.98379	7.91455
H	8.95587	19.38943	12.76349
H	7.36575	16.74601	15.84057
H	1.16572	15.20177	14.95772
H	2.90927	13.35618	11.41710
H	2.81770	21.29624	15.79763
H	0.84494	21.76208	11.94107

References

1) Liang, L.-C.; Chou, K.-W.; Su, W.-J.; Chen, H.-S.; Hsu, Y.-L.; Homo-and Heteropolynuclear Clusters of Phosphine Triphenolates. *Inorg. Chem.* **2015,** *54*, 11526-11534.

2) Nichols, A. W.; Chatterjee, S.; Sabat, M.; Machan, C. W.; Electrocatalytic reduction of CO_2 to formate by an iron schiff base complex. *Inorg. Chem.* **2018,** *57*, 2111-2121

3) Arnett, C. H.; Kaiser, J. T.; Agapie, T.; Remote Ligand Modifications Tune Electronic Distribution and Reactivity in Site-Differentiated, High-Spin Iron Clusters: Flipping Scaling Relationships. *Inorg. Chem.* **2019,** *58*, 15971-15982.

4) Bain, G. A.; Berry, J. F.; Diamagnetic corrections and Pascal's constants. *J. Chem. Educ.* **2008,** *85*, 532

5 (a) Becke, A. D. Phys. Rev. A 1988, 38, 3098. (b) Perdew, J. P. Phys Rev. B 1986, 33, 8822.

6) Weigand, F.; Ahlrichs, R. Phys. Chem. Chem. Phys. **2005,** 7, 3297